Civil and Project Journal, 2026, 8(8), 51-81
https://doi.org/10.22034/cpj.2026.585612.1448

Civil and Project Journal
http://www.cpjournals.com/

Investigating the simultaneous effect of roughness (toothed bed) and slope with a positive trend on the length and intensity of hydraulic jump in some normal hydraulic structures Review assessment

Amin. Aral [1], Roozbeh .Aghamajidi [2*]

1-MSC of Civil engineering , Sep. C., Islamic Azad University, Sep, Iran
2*- Department of Civil Engineering, Sep. C., Islamic Azad University, Sep, Iran

Received: 08 May 2026; Revised: 26 May 2026; Accepted: 10 June 2026; Published: 23 October 2026

ABSTRACT

Hydraulic jumps are a critical phenomenon in fluid mechanics, widely utilized in hydraulic engineering structures such as energy dissipation basins. These structures — including relaxation ponds located downstream of spillways, steep channels, and control valves — rely on the energy-dissipating characteristics of hydraulic jumps to manage and reduce the destructive force of fast-moving water before it continues downstream. To better understand the behavior and effectiveness of hydraulic jumps under various conditions, a series of controlled laboratory experiments were carried out. A total of 60 experimental runs were performed using a rectangular flume measuring 35 centimeters in width. The inlet Froude numbers tested ranged from 4 to 12, covering a broad spectrum of supercritical flow conditions. Throughout the study, two distinct types of bed roughness were examined — sharp corner roughness and diamond (rhombus) shaped roughness elements — both installed on the channel floor. In addition to roughness type, the longitudinal slope of the flume bed was systematically varied between 0% and 0.3% to assess its influence on jump characteristics. During each experimental run, several key hydraulic parameters were precisely recorded, including discharge rate, sequent depth ratio, jump length, water surface profile, flow depth upstream and downstream of the jump, and water head measurements at the weir crest. The findings of the study revealed meaningful differences in hydraulic jump behavior depending on the roughness configuration. Specifically, the presence of sharp corner roughness elements led to a notable reduction in the ratio of jump length to sequent depth — approximately 35.5% lower compared to a smooth bed. Furthermore, the sequent depth ratio increased by an average of 6.5% for sharp corner roughness. In contrast, diamond-shaped roughness showed a more modest influence, producing only a 1.2% average reduction in the jump length-to-sequent depth ratio

Keywords: *hydraulic jump, spillway, physical model, stilling basin, hydraulic jump, positive slope*

Cite this article as Aghamajidi,R and Aral,A . (2026). synergistic Effects of Bed Macroroughness and Positive Inclination on the Morpho dynamics and Energy Dissipation of Hydraulic JumpsAmin. (e245235). Civil and Project journal, 8(8), e245235 doi:8 https://doi.org/10.22034/cpj.2026.585612.1448 **ISSN:** 2676-511X / **Copyright:** © 2026 by the authors.

*Corresponding author E-mail address: *roozbehAghamajidi1396@gmail.com*

- **Introduction**:

Hydraulic jumps are among the most widely used and reliable processes for dissipating excessive kinetic energy in supercritical flows released downstream of hydraulic structures such as sluice gates, spillways, and weirs. In a typical stilling basin, the hydraulic jump transforms a fast, shallow supercritical stream into a slower, deeper subcritical flow. This abrupt transition is accompanied by intense turbulence, air entrainment, surface roller formation, and large-scale mixing, which together convert a substantial portion of the incoming kinetic energy into turbulence and heat. Because uncontrolled residual energy can lead to bed scour, structural undermining, and downstream instability, accurate prediction and enhancement of hydraulic-jump energy dissipation remains a central objective in stilling basin design and operation.While the free (or classical) hydraulic jump is often the target condition in stilling basins, field conditions commonly impose partial or full submergence due to high tailwater levels, downstream control structures, or backwater effects. Under such submerged conditions, the jump's internal structure and mixing mechanisms can change markedly. Rajaratnam (1965) showed that as the submergence ratio increases, turbulent mixing in the jump region progressively weakens and the overall energy dissipation becomes lower than that of a comparable free jump. A key physical manifestation of this behavior is the gradual suppression—and eventual disappearance—of the distinct high-velocity jet core that normally penetrates into the roller region and promotes strong entrainment and mixing (Rajaratnam, 1965). In other words, deeper submergence tends to "smooth" the jump, making it more stable in appearance but less efficient as an energy dissipator. To better describe the near-field hydraulics responsible for these trends, Rajaratnam and Subramanya (1967) examined the velocity and pressure fields immediately downstream of a deeply submerged sluice gate, providing detailed insight into how the jet, recirculation, and pressure recovery evolve when the gate outflow is forced beneath higher tailwater. Later, Ma et al. (2001) extended submerged-jump investigations through numerical modeling, demonstrating how computational approaches can reproduce key submerged-jump characteristics—such as velocity decay, pressure distribution, and reduced turbulence intensity—and can be used to explore parameter spaces that are difficult to test comprehensively in the laboratory (Ma et al., 2001). Collectively, these studies underline a practical design implication: when submergence is unavoidable, supplementary measures are often required to recover dissipation performance and maintain acceptable basin stability.

Table 1. Main hydraulic characteristics of free and submerged hydraulic jumps

Hydraulic feature	Free hydraulic jump	Submerged hydraulic jump
Surface roller development	Well-developed and clearly visible	Compressed or partially suppressed
Jet core behavior	Distinct, strong penetration into roller region	Gradually weakened and may disappear with increasing submergence
Turbulent mixing	Intense and highly effective	Reduced as submergence increases
Air entrainment	Significant	Lower due to suppression of surface turbulence
Energy dissipation efficiency	Generally high	Lower than in comparable free-jump conditions
Pressure recovery	Occurs through strong mixing and roller action	More gradual and influenced by tailwater control
Flow appearance	Highly turbulent and unstable-looking	Smoother and more stable in appearance
Design implication	Often preferred for stilling basins	May require supplementary dissipation devices

The comparison in Table 1 highlights the fundamental shift in hydraulic-jump behavior caused by submergence. Although submerged jumps may appear visually more stable because of reduced surface disturbance, this apparent stability is accompanied by weaker turbulence, lower air entrainment, and diminished dissipation efficiency. From a design perspective, this means that relying solely on tailwater-induced submergence may not provide adequate energy control in stilling basins. Instead, engineers often need to incorporate additional appurtenances—such as chute blocks, baffle blocks, or end sills—to compensate for the reduced mixing intensity and to ensure safe downstream flow conditions.

Use of appurtenances to improve stilling basin performance

Because the dissipative capacity of a conventional hydraulic jump can be compromised by submergence, sediment conditions, or geometric constraints, designers frequently incorporate appurtenances to enhance mixing, shorten jump length, and stabilize the roller location. Common passive countermeasures include: End sills, which help raise the sequent depth locally and promote roller stabilization; Intermediate sills and baffle blocks, which interrupt the supercritical jet, generate additional turbulence, and force stronger momentum exchange ; Roughness elements, which increase boundary shear and turbulence production and can reduce jump length. These devices effectively introduce controlled disturbances that intensify turbulence and redistribute momentum, thereby improving energy dissipation and often reducing the required basin length for safe operation.

Hydraulic jumps in abruptly expanding channels

Beyond appurtenances, basin geometry itself has been recognized as a major control on jump behavior. Many practical stilling basins and outlet channels exhibit changes in width due to site constraints, transitions, or energy-dissipation layouts. In abruptly expanding channels, the sudden lateral enlargement modifies pressure gradients, introduces strong lateral shear layers, and can lead to three-dimensional flow separation and asymmetric rollers. Smith (1989) investigated hydraulic jumps in abruptly expanding channels and highlighted how expansion affects jump formation and length. Bremen and Hager (1994) further clarified jump characteristics under expansion, strengthening predictive understanding for design in non-prismatic basins. Ohtsu et al. (1999) also contributed to this topic by examining how changes in channel geometry influence jump properties and energy loss mechanisms. More recently, Torkamanzad et al. (2019) performed laboratory experiments in an abruptly expanding asymmetric stilling basin. Their results suggested that intentional asymmetry—when combined with bed roughness measures—can be advantageous in certain operating ranges, for example by improving flow control, modifying recirculation patterns, and enhancing dissipation under specific tailwater and Froude number conditions (Torkamanzad et al., 2019). This line of work supports the broader conclusion that "non-classical" basin geometries can sometimes outperform conventional layouts when tailored to the site's dominant hydraulic regime.

Table 2. Summary of previous studies on hydraulic jumps in expanding and non-prismatic basins

Study	Basin/channel condition	Main focus	Key contribution
Smith (1989)	Abruptly expanding channel	Jump formation and jump length	Showed that lateral expansion significantly alters jump development and spatial extent
Bremen and Hager (1994)	Expanding/non-prismatic basin	Jump characteristics under expansion	Improved predictive understanding of jump behavior in widened basins
Ohtsu et al. (1999)	Variable channel geometry	Jump properties and energy loss	Demonstrated that geometric transitions influence dissipation mechanisms
Torkamanzad et al. (2019)	Abruptly expanding asymmetric stilling basin	Asymmetry, roughness, and flow control	Found that intentional asymmetry can improve dissipation and modify recirculation under certain conditions

Table 3. Hydraulic effects of basin expansion and asymmetry on jump behavior

Geometric feature	Hydraulic effect	Influence on jump behavior	Design implication
Abrupt width expansion	Sudden change in lateral pressure distribution	Alters jump position and increases complexity of roller structure	Requires revised jump-length and basin-sizing considerations
Lateral enlargement	Formation of shear layers	Promotes flow separation and three-dimensional motion	May reduce predictability of classical design equations
Non-prismatic geometry	Variable confinement of flow	Changes recirculation zones and energy-loss distribution	Can be used intentionally to tailor dissipation performance
Asymmetric basin layout	Uneven flow distribution across width	Produces asymmetric rollers and modified mixing patterns	May improve control under selected hydraulic conditions
Roughened bed with asymmetry	Added turbulence and resistance	Enhances dissipation and stabilizes flow in some regimes	Useful as a supplementary design strategy where suboptimal jumps occur

The two tables together show that basin geometry is not merely a secondary construction detail, but a governing parameter in hydraulic-jump performance. Table 1 summarizes the progression of research demonstrating that channel expansion, non-prismatic forms, and asymmetric layouts all have measurable impacts on jump structure and energy dissipation. Table 2 interprets these findings from a hydraulic-design perspective by linking specific geometric features to their flow consequences. Overall, the evidence suggests that while expanded and asymmetric basins may introduce greater flow complexity, they also offer opportunities for improving dissipation and flow regulation when designed in accordance with site-specific hydraulic conditions such as inflow Froude number, tailwater depth, and basin roughness.

Sensitivity to sill geometry and placement

The geometry and location of sills can strongly influence stilling basin efficiency, because these elements directly interact with the supercritical jet and the developing roller. Tiwari and Seema (2013, 2014) investigated basin configurations equipped with end sills and intermediate sills of different shapes and arrangements. Their findings emphasized that relatively small changes in sill geometry (e.g., height, crest shape) and placement (distance from the gate or basin entrance) can produce meaningful differences in jump stability, tailwater compatibility, and the fraction of energy dissipated (Tiwari & Seema, 2013, 2014). Practically, this means that sill design cannot be treated as a purely secondary detail; instead, it should be optimized in concert with the expected inflow Froude number range and tailwater variability.

Permeable screens as an alternative energy dissipation strategy

A distinct approach that has gained increasing attention is the placement of permeable screens downstream of the hydraulic structure. Unlike solid baffles, screens allow part of the flow to pass through, creating a distributed resistance that promotes turbulence generation and momentum exchange while avoiding the strong localized jets and cavitation-prone zones that can occur around solid obstacles. Experimental evidence has repeatedly shown that screen parameters—particularly porosity—govern their effectiveness.

Rajaratnam and Hurtig (2000) demonstrated that permeable screens can dissipate substantial energy when installed downstream of small hydraulic structures, and they identified a porosity on the order of about 40% as especially effective for energy reduction (Rajaratnam & Hurtig, 2000). Sadeghfam et al. (2015) reported similar conclusions, reinforcing the idea that porosity is a primary design variable controlling hydraulic resistance and turbulence production (Sadeghfam et al., 2015). From a physical standpoint, too low a porosity can behave like a near-solid barrier (potentially causing excessive afflux

https://doi.org/10.22034/cpj.2026.585612.1448

or unfavorable backwater), whereas too high a porosity may not generate sufficient resistance for strong dissipation. Hence, an intermediate porosity often yields the best balance between energy loss and hydraulic compatibility. Screen orientation has also been examined. Balkiş (2004) assessed whether inclining screens relative to the vertical improves performance and concluded that inclination produced no statistically significant gain in dissipation efficiency compared with vertical installation (Balkiş, 2004). This finding is important for practice because vertical screens are typically simpler to fabricate, install, inspect, and maintain.More systematic testing was carried out by Bozkuş and co-authors, who evaluated the combined influence of porosity (approximately 20%–60%), screen thickness, and longitudinal position within the basin. Their results indicated that, over a wide range of incoming Froude numbers, screen-equipped basins dissipated markedly more energy than a conventional hydraulic jump alone, and that screen location and thickness can meaningfully alter the dissipation outcome by changing how and where turbulence is generated (Bozkuş et al., 2008; Bozkuş et al., n.d.). Bozkuş and Aslankara (2008) further explored how tailwater depth interacts with multiple-screen arrangements, providing practically useful guidance for configurations where a single screen may not provide sufficient dissipation or where performance must be robust across varying submergence conditions (Bozkuş & Aslankara, 2008).Taken together, the literature indicates that although the hydraulic jump is a highly effective and economical energy dissipator in its free form, its performance can degrade substantially under strong submergence due to reduced turbulence and weakened mixing. As a result, modern stilling basin design increasingly relies on: (i) basin geometry optimization (including expansions and asymmetry), and (ii) strategically placed appurtenances such as sills, roughness elements, and particularly permeable screens whose porosity, thickness, and placement can be tuned for improved energy dissipation and operational stability. Continued integration of laboratory measurement, field observation, and numerical simulation remains essential for developing design guidance that is both physically grounded and robust for real-world tailwater variability.

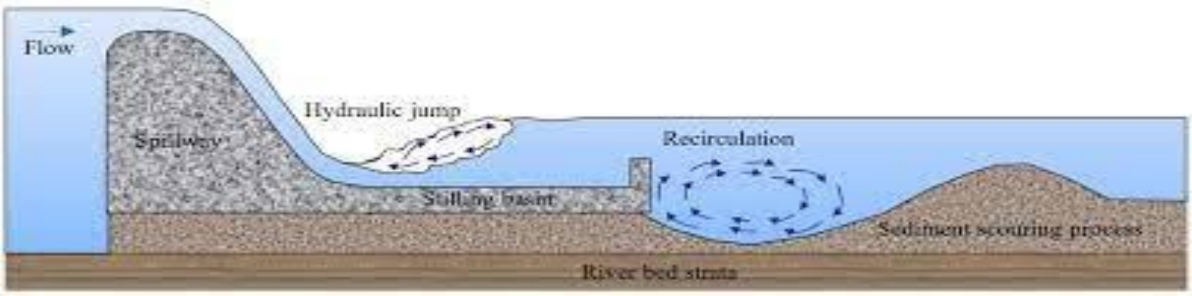

Figure 1: schematic view of hydraulic jump at stilling basin (with scouring in down stream)

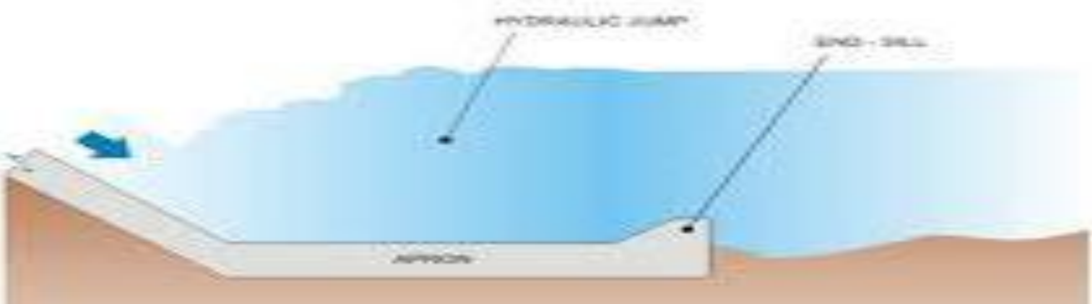

Figure 2: view of hydraulic jump at stilling basin (with successful dissipation on stilling basin)

The research surrounding hydraulic energy dissipation has evolved to consider the interplay between external flow conditions and internal basin configurations. Bozkuş and Aslankara (2008) conducted a pivotal investigation into how tailwater depth and the use of multiple screen arrangements affect energy dissipation performance. A significant finding of their work was that variations in tailwater depth did not appreciably alter the rate of energy dissipation. This suggests that screen-based dissipation systems offer a degree of hydraulic robustness, maintaining consistent efficiency even when downstream flow conditions fluctuate. Furthermore, their research demonstrated that configurations utilizing multiple screens were superior to a single screen setup, revealing a cumulative benefit where successive screens progressively strip kinetic energy from the flow (Bozkuş & Aslankara, 2008).Building upon the concept of structural interventions, researchers have also explored the utility of modified sills to control jump characteristics. Behrouzi-Rad et al. (2013) transitioned from thin screens to the study of perforated sills, analyzing the hydraulic properties of forced hydraulic jumps. By comparing these forced jumps to classical hydraulic jumps, the study provided quantitative evidence that perforated sills significantly modify the internal flow structure. The presence of perforations within the sill allows for a more complex interaction between the supercritical jet and the basin floor, which enhances energy loss while potentially reducing the risk of cavitation or extreme pressure fluctuations associated with solid, continuous sills (Behrouzi-Rad et al., 2013).The physical geometry of the openings within these dissipators has emerged as a critical design variable in recent years. Mahmoud et al. (2013) undertook a systematic study to determine how the specific shape of a screen’s pores influences its efficiency. By fixing porosity at 40%—a value previously identified as highly effective—they compared the performance of screens featuring circular holes against those with square holes in both single and double arrangements. Their results indicated a consistent performance advantage for square-holed screens. This suggests that the sharper edges and specific wake patterns generated by square apertures promote more intense turbulent mixing and higher head loss than the smoother flow paths facilitated by circular openings (Mahmoud et al., 2013).Further exploration into porosity levels and hole geometry was conducted by Abbaspour et al. (2019), who focused on screens with a 50% porosity and square hole configurations. This research refined the understanding of how the interaction between the percentage of open area and the shape of the void governs the overall hydraulic response. By testing higher porosity levels with square geometries, the study helped delineate the threshold at which porosity facilitates sufficient flow passage while still maintaining enough resistance to maximize energy dissipation. Such findings are vital for engineers who must balance the need for high dissipation rates with the requirement to prevent excessive backwater effects or structural clogging (Abbaspour et al., 2019).Collectively, these studies underscore that the optimization of energy dissipation in stilling basins is a multi-parameter challenge. The evidence suggests that while classical jumps are limited by their environment, engineered solutions like multiple permeable screens and perforated sills provide more controllable and efficient outcomes. By carefully selecting parameters such as porosity, hole shape (specifically square over circular), and the number and spacing of screens, designers can tailor hydraulic structures to remain effective across a broad spectrum of Froude numbers and tailwater conditions. This body of research establishes a clear framework for the next generation of high-efficiency, passive energy-dissipating systems in hydraulic engineering.

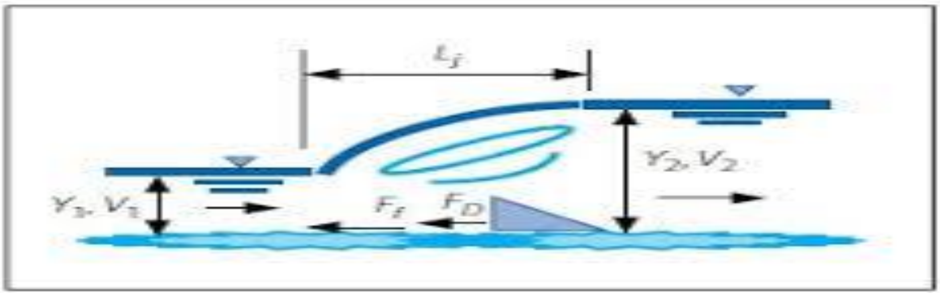

Figure 3: schematic view of hydraulic jump at theory

The geometric configuration of hydraulic structures plays a pivotal role in determining the efficiency of energy dissipation in open channels. Experimental data indicates that screens positioned on an adverse slope of 0.0250.0250.025 demonstrate a significantly higher capacity for dissipating energy compared to those on a milder slope of 0.0150.0150.015. This suggests that the gravitational resistance provided by a steeper adverse slope enhances the turbulence and friction loss within the flow. Furthermore, the spatial arrangement of these screens is a critical factor; double-screen configurations consistently outperform single-screen setups. This improved performance is attributed to the creation of secondary turbulence zones and increased drag, which more effectively break down the kinetic energy of the supercritical flow. Building upon structural interventions, the utilization of perforated sills has proven to be a highly effective method for controlling hydraulic jumps. Research conducted by Fathi-Moghadam et al. (2017) focused on the “B-type” hydraulic jump, revealing that both the presence and the specific positioning of a perforated sill are instrumental in energy reduction. These sills act as physical barriers that force flow separation and promote the rapid development of the jump over much shorter distances than would occur naturally. By optimizing the sill's location, engineers can significantly reduce the length of the required downstream protection, thereby minimizing construction costs while maintaining structural safety.

Table 4: Comparative Effects of Slope and Arrangement on Energy Dissipation

Variable Category	Configuration Type	Energy Dissipation Efficiency	Impact on Flow Velocity
Adverse Slope	0.015 Gradient	Moderate	Lower Reduction
Adverse Slope	0.025 Gradient	High	Significant Reduction
Screen Setup	Single Arrangement	Baseline	Standard Drag
Screen Setup	Double Arrangement	Enhanced	High Turbulence/Drag

The data summarized in Table 1 highlights the sensitivity of hydraulic energy loss to the physical orientation of the channel bed and the density of the screen obstacles. An adverse slope essentially forces the water to work against gravity, and as the gradient increases from 0.0150.0150.015 to 0.0250.0250.025, the energy required for the fluid to pass through the screen increases, leading to a higher dissipation rate. This relationship is especially important for designers who need reliable ways to manage high-velocity flows in steep channels or in the reach immediately downstream of spillways. When the configuration shifts from a single screen to a double-screen arrangement, the hydraulics become more complicated because the outflow and wake generated by the first screen directly influence how water approaches and passes through the second screen. In effect, the system operates through a "double-hit" mechanism: energy that is not sufficiently dissipated by the first barrier is further reduced by the second. This interaction typically leads to a higher overall drag coefficient and stronger, more persistent eddy formation between and downstream of the screens—two key reasons why double-screen layouts often outperform single-screen systems in terms of energy dissipation and flow control.Alongside laboratory testing, numerical modeling has become an essential tool for investigating the detailed flow structures around perforated barriers. Daneshfaraz et al. (2017), for example, used Reynolds-Averaged Navier–Stokes (RANS) simulations to study how supercritical flow interacts with perforated screens. This type of computational modeling makes it possible to observe localized three-dimensional features—such as recirculation zones, turbulence production, and velocity gradients near the openings—that are difficult to measure accurately in physical models. Based on their analyses, they developed a set of predictive equations to estimate the relative depth of hydraulic jumps passing through perforated screens. These equations provide a practical framework for hydraulic design by improving the ability to predict jump characteristics and downstream flow behavior under different screen configurations.Screen geometry has also been expanded beyond simple vertical layouts to include V-shaped designs, which can offer distinct hydraulic benefits. Zayed et al. (2018) investigated triangular V-shaped screens and examined how parameters such as apex angle, blockage ratio, and the use of circular bars affect performance. Their results showed a clear positive relationship between head loss and blockage ratio: as the proportion of the flow area obstructed by the screen increases, energy losses increase as well. They also found that, for screens constructed with circular bars, smaller screen angles could reduce head loss. This suggests that the bar shape and its hydrodynamic profile significantly influence resistance and flow separation, and that streamlined elements may dissipate energy more efficiently while avoiding excessive upstream losses.

Finally, Daneshfaraz et al. (2019) extended this line of research to movable-bed conditions, demonstrating that screen-driven energy dissipation can strongly affect sediment transport processes and downstream bed stability. By modifying turbulence levels, near-bed velocities, and recirculation patterns, perforated screens can either promote deposition or intensify local scour depending on the design and flow conditions. These findings highlight that perforated screen systems are not only valuable for reducing flow energy, but also for managing erosion risk and maintaining channel stability in sediment-laden environments.

Table 5: Key Research Contributions in Hydraulic Screen Analysis

Researcher(s)	Focus Area	Primary Finding	Methodology
Fathi-Moghadam (2017)	Perforated Sills	Sills shorten B-type jump distance significantly.	Experimental
Daneshfaraz et al. (2017)	RANS Modeling	Developed equations for relative jump depth.	Numerical (CFD)
Zayed et al. (2018)	V-shaped Screens	Head loss increases with blockage and discharge.	Experimental
Daneshfaraz et al. (2019)	Movable Beds	Screens protect bed stability downstream.	Experimental

Table 5 categorizes the evolution of research in this field, showing a clear progression from basic energy dissipation studies to complex three-dimensional numerical simulations. The work by Fathi-Moghadam and Zayed emphasizes the physical geometry of the structures—sills and V-shapes—demonstrating that altering the shape and angle of a barrier can tune the hydraulic response of the system. This allows for customized engineering solutions based on the specific discharge requirements of a site.The inclusion of the 2017 and 2019 studies by Daneshfaraz highlights the duality of modern hydraulic research: the use of RANS equations to provide theoretical depth and the application of those theories to real-world scenarios like movable bed protection. By understanding how perforated screens interact with supercritical flow at a molecular and mathematical level, researchers can better predict how these same screens will prevent erosion and scour in natural riverbeds, bridging the gap between fluid mechanics and environmental engineering.

Table 6: Factors Influencing Head Loss and Flow Characteristics

Factor	Change in Variable	Effect on Head Loss (HLH_LHL)	Effect on Jump Length (LjL_jLj)
Blockage Ratio	Increase	Increase	Decrease
Flow Discharge	Increase	Increase	Increase
Screen Angle (V-shape)	Decrease	Decrease	Variable
Sill Position	Optimization	Moderate	Significant Decrease

Table 6 serves as a design guide for the operational variables discussed in the research. It illustrates that the blockage ratio is perhaps the most influential parameter for increasing head loss. By increasing the area of the screen that obstructs the flow, the fluid is forced through smaller apertures at higher velocities, creating significant pressure drops and energy conversion. This is the primary mechanism used to transform high-energy supercritical flow into more manageable subcritical flow.The table also reflects the findings regarding V-shaped screen angles and sill positioning. While increasing discharge naturally increases head loss due to higher volumes of water interacting with the barriers, the "Screen Angle" variable shows that the geometry can be used to mitigate or enhance this effect. For instance, in circular bar designs, a lower angle allows for a more streamlined flow, which can be useful when some energy preservation is required. Conversely, the strategic placement of a sill is the most effective way to minimize the length of the hydraulic jump, ensuring the transition occurs within a controlled, reinforced section of the channel.

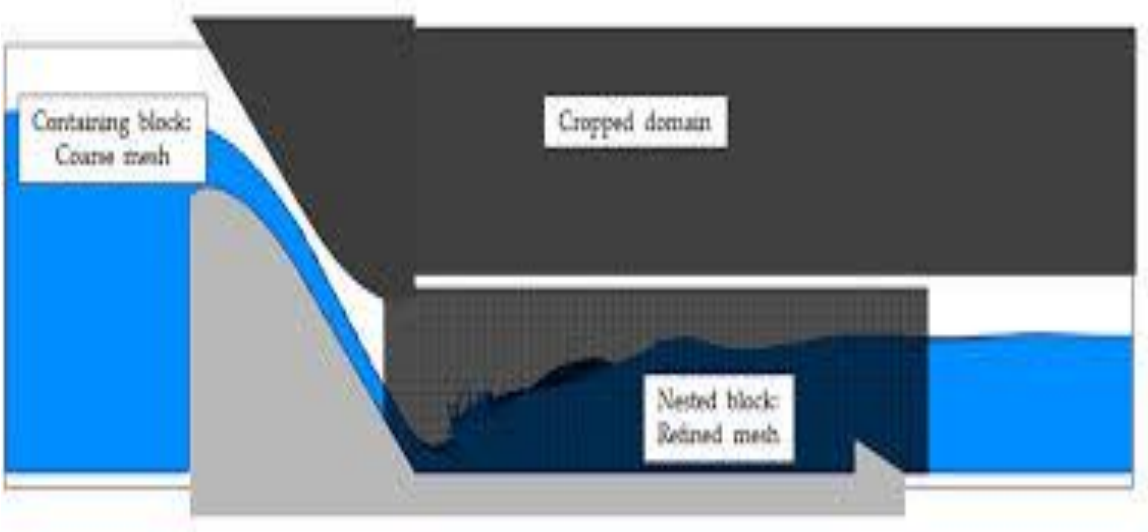

Figure 4: schematic view of hydraulic jump at downstream of diversion dams

experiments were conducted using screen systems arranged in both single and double configurations, with porosity levels of 40% and 50%, and tested over three different bed-material (particle) sizes. The results indicated that the maximum energy dissipation occurred when a double-screen arrangement with 40% porosity was used, suggesting that the combined resistance of two lower-porosity barriers intensifies turbulence and momentum loss. In contrast, when maintaining a constant level of energy dissipation, the single-screen configuration with 50% porosity generated the least bed scour, implying that a more open screen can reduce near-bed shear stress and sediment mobilization while still providing adequate dissipation. Related laboratory work on scour caused by supercritical flow impinging on screens was presented by Sadeghfam et al. (2019). Their study emphasized how the interaction between high-velocity flow and screen elements can produce localized turbulence and bed degradation downstream. These findings support the broader understanding that both screen geometry (e.g., porosity and arrangement) and bed characteristics (grain size) strongly govern the extent of scouring and the effectiveness of energy dissipation in stilling basins (Sadeghfam et al., 2019).The primary purpose of the present study is to experimentally evaluate the hydraulic performance of a vertical screen installed within a sudden-expansion stilling basin. Specifically, the research examines how the screen modifies the behavior of a submerged hydraulic jump and how it influences downstream energy dissipation immediately after the vertical gate. By placing the screen within an expanding basin, the study targets a practical design condition where flow deceleration and jump stabilization are required in a limited space, such as downstream of gates, regulators, and spillway outlets.In addition to the laboratory observations, the study seeks to formulate theoretical (predictive) models for the hydraulic response of the system. These models are intended to provide designers with usable relationships for selecting the most effective auxiliary components—such as screen porosity, number of screens, and placement relative to the gate and basin expansion—to achieve an optimal balance between energy dissipation and scour control. In this way, the combined experimental and analytical outcomes can be used to improve stilling-basin design efficiency and reduce downstream erosion risks.

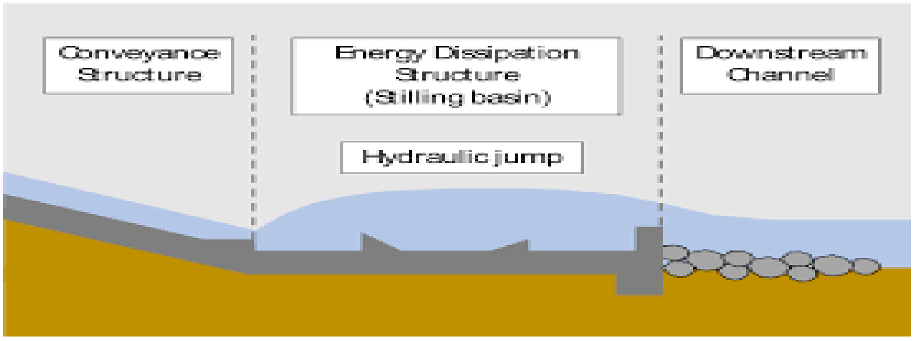

Figure 5: schematic view of smooth hydraulic jump in stilling basin

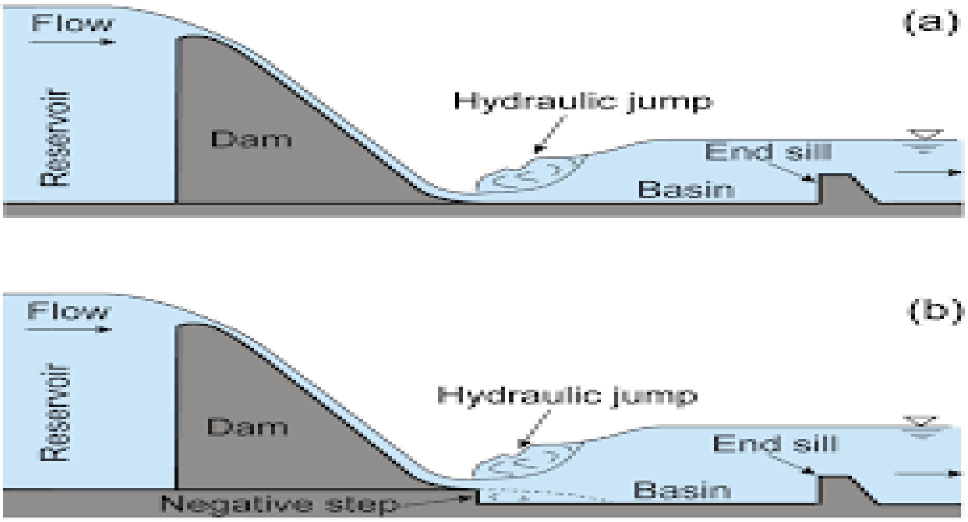

Figure 6 : schematic view of the different hydraulic jump condition in the in stilling basin

Literature review:

A **hydraulic jump** is a rapidly varied flow phenomenon that takes place when water flowing at **supercritical conditions** transitions to **subcritical flow**. During this transition, a large portion of the flow's kinetic energy is converted into turbulence, air entrainment, and heat, making the hydraulic jump one of the most effective natural mechanisms for **energy dissipation** downstream of hydraulic structures. Because of this property, hydraulic jumps are deliberately utilized in the design of **stilling basins**, spillways, sluice structures, barrages, and outlet works to reduce destructive velocities and protect downstream beds and structures from erosion and cavitation.

The behavior of a hydraulic jump is commonly described using the **upstream Froude number**, Fr1. Based on Bélanger's classical analysis the momentum equation can be simplified to estimate the **sequent depth ratio**, which links the initial depth before the jump to the conjugate depth after the jump. The value of the Froude number also provides a practical basis for classifying jumps according to their appearance and stability. In general, hydraulic jumps may be grouped into four major classes: **weak jumps** for $1.7<Fr1<2.5$**oscillating jumps** for $2.5<Fr1<4.5$, **steady jumps** for $4.5<Fr1<9$and **strong jumps** for $Fr1>9$as reported by Murzyn and Chanson (2009). Each category exhibits distinct flow patterns, roller behavior, turbulence intensity, and energy dissipation characteristics.

Over the years, numerous **experimental** and **numerical** studies have been carried out to improve understanding of hydraulic jump dynamics. Several investigations have focused particularly on free-surface fluctuations, turbulence structure, velocity distribution, and air entrainment. For example, **Wang and Chanson (2015)** performed experiments to analyze the fluctuating behavior of the free surface within hydraulic jumps. Likewise, **Chachereau and Chanson (2011)** and **Murzyn and Chanson (2009)** examined both velocity fluctuations and free-surface motion in the jump region. Their findings showed that intense turbulent fluctuations are present even upstream of the main roller, and spectral analyses of the free surface identified characteristic frequencies generally ranging from **1.4 to 4 Hz**.

Similarly, **Longo (2010, 2011)** conducted laboratory investigations in a flume to study turbulence beneath the free surface in stationary flows generated by a **Crump weir**. In those experiments, an **ultrasonic distance sensor** was used to measure free-surface variations, while an **ultrasonic Doppler velocity profiler** was employed to capture the velocity field. The results indicated that the free-surface elevation spectrum exhibited a dominant peak near **2 Hz**, and this peak was influenced by changes in the Froude number. Longo further observed that at relatively low Froude numbers the free surface remained comparatively smooth, with reduced turbulence and weaker velocity fluctuations. At intermediate Froude numbers, however, the boundary layer became thicker and the surface fluctuations increased, indicating more intense hydraulic jump behavior within the channel flow.

The internal structure of hydraulic jumps has also been explored from the standpoint of **air entrainment and bubbly flow behavior**. For instance, **Kucukali and Chanson (2008)** investigated the distribution and characteristics of bubbles within hydraulic jumps, providing useful insight into aeration processes and multiphase flow interactions. Other researchers examined the influence of channel modifications on jump properties. **Hager and Li (1992)** conducted experiments in a rectangular channel to evaluate how continuous and transverse sills affect hydraulic jump characteristics. In another study, **Hager and Bremen (1989)** assessed the influence of wall effects and reported that the **sequent depth** of a classical hydraulic jump is sensitive to the incoming Reynolds number, indicating that viscous and boundary-related effects can alter jump geometry and performance.

The effectiveness of hydraulic structures such as **dams, spillways, barrages, and outlet conduits** is closely associated with the geometry and hydraulic efficiency of the **stilling basin**. The main purpose of a stilling basin is to contain the hydraulic jump and dissipate the residual energy of the high-velocity flow released from upstream structures. If this energy is not adequately reduced, severe downstream problems may occur, including **bed scour, bank erosion, cavitation damage, structural vibration, and failure of protective works**. Therefore, suitable arrangements such as **baffle blocks, chute blocks, sills, end thresholds, and aprons** are commonly introduced to stabilize the jump at a desired location and improve energy dissipation.

Even after the jump forms within a stilling basin, some amount of residual energy usually remains in the downstream flow. To address this, designers often provide additional protection measures such as **flexible aprons, riprap, or launching aprons** downstream of the basin. These features help absorb remaining turbulence and protect the riverbed from local scour. Because of the critical role of stilling basins in hydraulic safety, many researchers have devoted considerable attention to improving their design and performance under varying flow and tailwater conditions.

Among recent studies, **Bantacut et al. (2022)** experimentally evaluated energy dissipation in a **USBR-IV stilling basin** after modifying the configuration of the energy dissipators, floor elevation, end sill, and riprap length. Their results demonstrated that the modified basin performed better than the original design. Specifically, energy dissipation increased from **89.5% to 98.4%** under the Q2discharge condition and from **77.7% to 84.8%** under the Q1condition. These findings highlight the importance of geometric optimization in stilling basin design.

In another study, **Aydogdu et al. (2022)** used **ANSYS Fluent** to numerically investigate the influence of different central sill shapes in an expanding stilling basin. Their computational results were compared with laboratory measurements and showed good agreement, confirming the usefulness of CFD tools for examining design alternatives. **Ali and Kaleem (2015)** studied the energy dissipation performance of the stilling basin at **Taunsa Barrage** in Punjab, Pakistan, before and after remodeling. Their investigation concluded that the remodeling strategy was not hydraulically appropriate, as it contributed to the launching of the stone apron and promoted river migration toward the left side of the barrage.

Related work by **Chaudhry (2010a)** reviewed the hydraulic performance of Taunsa Barrage stilling basins under different discharge conditions and **tailwater levels (TWLs)**. The analysis indicated that the tailwater levels considered in the original barrage design were sufficient for the formation of stable hydraulic jumps. The study also pointed out that the hydraulic behavior of the basin changed significantly after remodeling. Similarly, **Chaudary and Sarwar (2014)** examined the hydraulics of the old and modified stilling basins at Taunsa Barrage under both design and altered tailwater conditions. Their results suggested that the remodeled basin dissipated less energy than the original one, even though the available tailwater levels remained adequate for hydraulic jump formation. They further observed that the construction of a **sub-weir** downstream of the main structure led to sediment deposition between the two hydraulic controls.

In addition to physical modeling, **numerical simulation** has become an essential approach for investigating complex flow behavior in stilling basins and hydraulic jumps. Because these flows are highly turbulent, three-dimensional, and often involve air entrainment and recirculation, many details are difficult or impossible to measure experimentally. Advances in computational methods and computer hardware have enabled engineers to study such flow fields with much greater resolution and efficiency. As noted by **Siuta (2018)**, modern computational tools provide hydraulic engineers with strong capabilities for solving practical design problems through turbulence modeling.

A range of **turbulence models** has been used to simulate hydraulic jumps and stilling basin flows. Among the most commonly applied are the two-equation models such as the **standard k−εk-\varepsilonk−ε** model, the **RNG k−ε** model, and several **hybrid turbulence approaches**. According to **Carvalho et al. (2008)** and **Wang et al. (2016)**, these models are particularly valuable for representing complicated flow features that are difficult to capture in laboratory studies alone. They can provide insight into the internal flow structure, including recirculation zones, turbulent shear layers, pressure fields, and air entrainment processes, as also discussed by **Chanson and Gualtieri (2008)**.

In current hydraulic engineering practice, software packages such as **FLOW-3D**, **ANSYS Fluent**, and **Open FOAM** are widely used for analyzing hydraulic structures and stilling basin performance. These programs divide the flow domain into numerous computational cells and solve the discretized **Navier–Stokes equations** throughout the grid. Through this numerical framework, engineers can predict velocity distribution, pressure variation, turbulence intensity, jump length, roller formation, and energy dissipation efficiency for different structural configurations. As explained by **Bayon-Barrachina et al. (2015)**, such discretization-based numerical techniques have become highly effective tools for optimizing hydraulic designs and evaluating alternative arrangements before construction.

Overall, both laboratory experimentation and computational fluid dynamics have made significant contributions to the understanding of **hydraulic jump mechanisms** and the **hydraulic performance of stilling basins**. Experimental studies offer direct observations of turbulence, free-surface oscillation, and air-water interaction, while numerical approaches provide detailed spatial information that may not be accessible through measurements alone. Together, these methods support safer and more economical hydraulic structure design by improving the prediction of energy dissipation, jump stability, and downstream flow behavior.

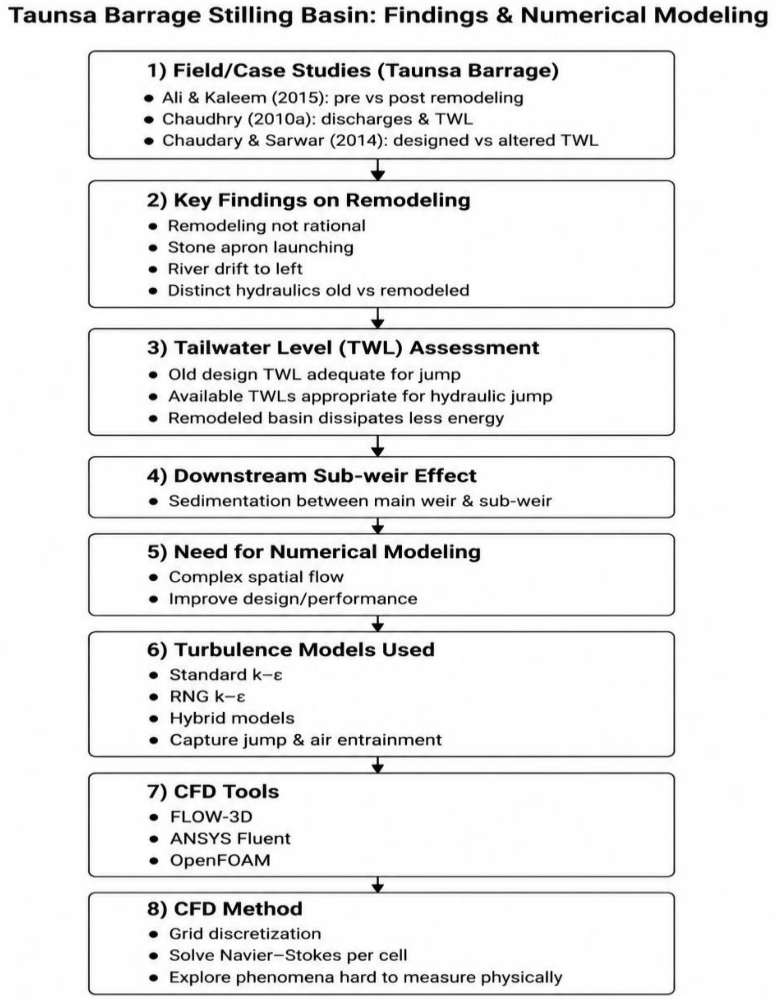

Figure (7) Flowchart of Experimental and Numerical Investigations on Stilling Basin Hydraulics

Recent progress in computational fluid dynamics (CFD) has significantly enhanced the ability to analyze the complex behavior of hydraulic jumps under different flow conditions. Various researchers have employed advanced numerical tools to simulate and examine the flow structure, turbulence characteristics, and energy dissipation mechanisms associated with hydraulic jumps. For instance, Bayon-Barrachina and Lopez-Jimenez (2015) utilized OpenFOAM to model classical hydraulic jumps in prismatic rectangular channels, providing detailed insight into flow patterns and surface fluctuations. Expanding on such approaches, Mukha et al. (2022) adopted a Large Eddy Simulation (LES) framework within OpenFOAM to capture the turbulent nature of hydraulic jumps and conducted comparisons with Direct Numerical Simulation (DNS), highlighting the effectiveness of LES in resolving transient flow features. In parallel, FLOW-3D has also been widely applied; Nikmehr and Aminpour (2020) used it to study hydraulic jumps over rough beds, confirming the reliability of numerical outputs through experimental validation. Similarly, Mirzaei and Tootoonchi (2020) integrated experimental measurements with FLOW-3D simulations to evaluate the impact of sluice gates and bed modifications on jump behavior across a range of hydraulic scenarios. Other contributions, such as Macián-Pérez et al. (2020), focused on quantifying key hydraulic parameters including free-surface profiles, sequent depth ratios, and energy dissipation efficiency, while Carvalho et al. (2008) demonstrated the applicability of the VOF method combined with the RNG k–ε$k–\varepsilon$ turbulence model in accurately predicting velocity and pressure fields.

In addition to three-dimensional CFD models, simplified numerical tools have also been employed to assess hydraulic performance in large-scale structures. Chaudhry (2010b) implemented the HEC-RAS model to analyze flow characteristics within the stilling basins of Taunsa Barrage, with particular attention to parameters such as tailwater levels, velocity distributions, Froude numbers, and hydraulic jump positions. The analysis indicated that, under the original design configuration, the hydraulic jump was effectively contained within the stilling basin and flow velocities remained within acceptable safety limits. However, after structural modifications, the hydraulic conditions changed considerably, leading to an increase in flow depth and a shift of the hydraulic jump toward the upstream glacis. This upstream migration suggests a reduction in energy dissipation efficiency and raises concerns regarding potential structural instability and operational safety.

Barrages are critical hydraulic infrastructures in Pakistan, serving as key components of irrigation systems that support extensive agricultural activities. Despite their importance, many barrages have experienced progressive deterioration due to factors such as aging infrastructure, hydraulic inefficiencies, structural weaknesses, and sedimentation or retrogression processes, all of which threaten their functionality and long-term stability (ICR, 2010). Taunsa Barrage, situated on the Indus River in Punjab, represents one of the major diversion structures in the region. It was originally designed with a modified United States Bureau of Reclamation (USBR) Type III stilling basin to safely accommodate a design discharge of 28,313 m3/s28,313m3/s. Soon after its commissioning, the barrage encountered multiple hydraulic and structural challenges, necessitating a series of temporary repair measures. Ultimately, a comprehensive rehabilitation program was executed between 2005 and 2008, during which the geometry of the stilling basin was significantly altered in an attempt to improve its performance.

A review of existing literature reveals that only a limited number of studies have systematically evaluated the hydraulic performance of Taunsa Barrage before and after its rehabilitation (Chaudhry, 2010a, 2010b; Chaudhary & Sarwar, 2014; Ali & Kaleem, 2015). These studies primarily focused on assessing the influence of tailwater levels on hydraulic jump formation and overall basin performance. Their findings generally indicate that post-rehabilitation conditions resulted in reduced efficiency, including issues such as the displacement of stone aprons and failure of inverted filter layers, which point to inadequate energy dissipation. However, there remains a noticeable gap in the literature regarding the quantitative assessment of critical hydraulic parameters, including free-surface profiles, flow depths, velocity distributions, hydraulic jump roller lengths, energy dissipation efficiency, and turbulent kinetic energy (TKE). To address this gap, the present study employs FLOW-3D to perform a detailed numerical investigation of flow behavior under a discharge of 44 m3/s44m3/s (gated flow) for both the original and remodeled stilling basin configurations of Taunsa Barrage. The study aims to comprehensively evaluate the effects of varying tailwater conditions on key hydraulic characteristics, including FSP, flow depth, Froude number, roller length, velocity field, energy dissipation efficiency, and TKE, thereby providing a more in-depth comparison of the two designs.

Table 7. CFD and 1D/2D Modeling Studies on Hydraulic Jumps and Stilling Basins

Study (Year)	Software / Solver	Model / Approach	Main Focus / Outputs
Bayon-Barrachina & Lopez-Jimenez (2015)	OpenFOAM	Numerical CFD	Classical hydraulic jump characteristics in a rectangular prismatic channel
Mukha et al. (2022)	OpenFOAM	LES; compared with DNS	Hydraulic parameters of classical jump; evaluation of LES performance versus DNS
Nikmehr & Aminpour (2020)	FLOW-3D	CFD (validated with lab data)	Effects of rough bed on hydraulic jump behavior
Mirzaei & Tootoonchi (2020)	Experiments + FLOW-3D	Physical model + CFD validation	Effects of sluice gate and bump on jump characteristics under different conditions
Macián-Pérez et al. (2020)	FLOW-3D	CFD	Jump structure: shape, free-surface profile (FSP), sequent depth ratio, and efficiency
Carvalho et al. (2008)	FLOW-3D	VOF + RNG kkk–ε\varepsilonε	Pressure/velocity profiles; comparison of CFD results with experiments
Chaudhry (2010b)	HEC-RAS	1D surface flow analysis	Tailwater, velocity, Froude number, and jump location in original vs. remodeled Taunsa basin

Table 4 consolidates the modeling literature cited in your text and shows how different numerical tools have been applied to hydraulic jumps. OpenFOAM studies range from general CFD investigations to advanced turbulence approaches (e.g., LES benchmarked against DNS), while FLOW-3D is frequently used for practical hydraulic engineering evaluations, including rough-bed effects and detailed structural characterization (FSP, sequent depth, efficiency). HEC-RAS is presented as a complementary 1D tool used to assess basin-wide surface-flow indicators (tailwater, velocity, jump location), especially useful for operational comparisons such as “original vs. remodeled” stilling basin performance.

Table 8. Context: Barrages in Pakistan and Rehabilitation Background of Taunsa Barrage

Item	**Summary from Text**	**Engineering Implication**
Importance of barrages	Supply irrigation water to large agricultural areas in Pakistan	Operational reliability and safety are critical for food/water security
Common problems reported	Aging; hydraulic issues; structural distress; sedimentation/retrogression (ICR, 2010)	Can threaten stability and require rehabilitation or redesign of dissipators/basins
Taunsa Barrage location and role	Major diversion structure on the Indus River (Punjab, Pakistan)	High discharge variability and sediment load demand robust energy dissipation
Original stilling basin type	Modified USBR Type-III	Basin configuration intended to stabilize jump and control scour at design flows
Design discharge	28,313 m3/s28{,}313\ \text{m}^3/\text{s}28,313 m3/s	Large design discharge implies extreme energy and scour potential
Rehabilitation timeframe	2005–2008 (after recurring issues and partial repairs)	Geometric changes can alter jump location, depth, and apron performance
Changes during rehabilitation	Remodeling of stilling basin with geometric modifications	Can shift hydraulic regime and affect safety margins (e.g., jump moving onto glacis)

Table 5 summarizes the infrastructure and hydraulic setting that motivates the study. The text emphasizes that Pakistan's barrages are essential but increasingly vulnerable due to age, hydraulics, structural deterioration, and sediment-related processes. Taunsa Barrage is highlighted as a critical case where a modified USBR Type-III basin was originally designed for very large discharge, yet post-construction problems led to major rehabilitation and basin geometry changes. These changes are important because even modest geometric modifications can significantly influence hydraulic jump stability, tailwater compatibility, and the survivability of downstream protective works.

Table 9. Research Gap and Objectives of the Present FLOW-3D Study (Taunsa Barrage)

Category	Details from Text
Prior Taunsa-related studies cited	Chaudhry (2010a, 2010b); Chaudary & Sarwar (2014); Ali & Kaleem (2015)
What those studies mainly addressed	Review of previous reports; effects of tailwater levels (TWLs) in original vs. remodeled basins; qualitative/operational performance outcomes
Reported post-remodeling issues	Stone apron and inverted filter blocks washed away (as indicated by literature)
Key gap identified	Limited quantification of hydraulic parameters (FSP, flow depth, velocity profile, roller length, jump efficiency, turbulence kinetic energy) for both basins
Present study method	FLOW-3D numerical modeling
Flow condition investigated	44 m3/s44\ \text{m}^3/\text{s}44 m3/s (gated flow)
Main comparison variable	Tailwater changes and their influence on jump behavior
Parameters evaluated	FSPs, flow depth, Froude number, roller length, velocity, hydraulic jump efficiency, TKE
Overall aim	Compare flow behavior in Taunsa stilling basins before vs. after remodeling

Table 6 translates your problem statement into a structured "gap-to-objective" summary. While earlier work on Taunsa Barrage largely focused on tailwater adequacy, jump location trends, and qualitative performance before/after rehabilitation, the text notes a lack of detailed, parameter-by-parameter quantification—particularly for free-surface profile development, internal velocity structure, roller length, efficiency metrics, and turbulence measures such as TKE. The present study addresses this by using FLOW-3D to model a representative gated-flow discharge (44 m3/s44\ \text{m}^3/\text{s}44 m3/s) and systematically comparing how tailwater changes affect hydraulic-jump indicators in the two basin geometries.

- **Materials and methods**

The experiments were carried out in the laboratory flume of the Hydraulic Laboratory, Yasouj Azad University. The flume is 8.0 m long, 0.35 m wide, and 0.40 m deep (Figure 1). The bed (floor) of the channel is made of Plexiglas, while the sidewalls are glass to provide adequate visibility for flow observation. The upstream supply tank (head tank) is also fabricated from Plexiglas, with an approximate storage capacity of 1.0 m^3. Plexiglas was selected for the flume body in accordance with USBR (U.S. Bureau of Reclamation) recommendations, due to its smooth surface, dimensional stability, and suitability for hydraulic modeling and visual inspection. To generate controlled boundary roughness on the flume floor, rhombus-shaped roughness elements manufactured from Teflon were used. Teflon roughness was chosen because it offers good durability, stable geometry under repeated testing, and consistent surface properties, helping to ensure repeatability of the experiments. A key consideration in installing the roughness elements was to avoid adverse flow behavior such as separation of streamlines and the initiation of cavitation, particularly in the high-velocity region where supercritical flow forms. For this reason, the roughness elements were mounted so that their upper surfaces were aligned (flush) with the surface elevation of the spillway toe/crest transition region where the supercritical flow is generated. This alignment helps prevent the creation of abrupt steps or protrusions that could cause local pressure drops, flow detachment, and strong vortical structures. The geometric and arrangement characteristics of the roughness elements used on the bed are summarized in Table (1). In general, the primary roughness parameters include:

- **Roughness height (k):** the vertical projection of the element above the reference bed level (i.e., the effective roughness height controlling momentum loss and turbulence generation).
- **Roughness width (b):** the lateral dimension of each rhombic element measured perpendicular to the flow direction.
- **Covered length (Lc):** the streamwise length of the bed section occupied by the roughness elements (i.e., the total roughened reach along the flume).

Accordingly, in this study the **roughness height** represents the element elevation responsible for altering the near-bed velocity profile and increasing turbulence intensity, while the **roughness width** and **covered length** define the plan-area coverage and the extent of the roughened zone. These parameters collectively control the degree of energy dissipation, boundary shear modification, and flow resistance induced by the rhombic roughness pattern.

If it be seen Table (10) (values of height, width, spacing, and covered length), I can rewrite this section in a more formal journal style and explicitly tie the dimensions to standard roughness descriptors (e.g., relative submergence k/h, roughness density/coverage ratio, and spacing ratios).

Table 10: Characteristics of rhombus roughness used in the research

Rough number	Roughness width(mm)	roughness length in flow direction(mm)	Roughness height(mm)	rough shape
1	**no roughness**			
2	22.6	16	16	**Diamond**

Figure 8: Laboratory flume for experimental tests

Accurate flow-depth measurement in the hydraulic-jump zone is challenging because the free surface is strongly aerated, highly turbulent, and spatially non-uniform. To obtain representative sequent depths, the primary and secondary depths were therefore not taken from a single point reading. At every target cross-section, three independent depth readings were collected—one along the channel centerline and two close to the sidewalls—and their arithmetic mean was adopted as the section depth. Averaging in this way helps suppress the influence of local surface oscillations, cross-waves, and near-wall effects, yielding a more stable estimate of the mean water depth within the jump. For each experimental run, a set of key variables was measured directly to characterize the hydraulic conditions and the jump geometry. These measurements included the discharge QQQ passing through the flume; the initial jump depth y1 immediately upstream of the roller (supercritical approach flow); and the sequent depth y2downstream of the jump once the flow had transitioned to a comparatively stable subcritical regime. Additional depth and length scales were also recorded: the toe (or footing) depth TWTWTW at the location where the jump initiates; the hydraulic-jump length Lj defined from the toe to the section where the water surface becomes approximately uniform; and the roller length L remeasured from the toe to the end of the visibly recirculating surface roller (where surface boils and roller effects largely disappear).

To define the upstream driving head and the boundary conditions governing jump formation, the head over the spillway crest HHH was measured relative to the crest elevation at the overflow section, and the upstream water level (approach head/water load) was recorded to describe incoming flow conditions prior to overflow. The evolution of the jump was further documented by surveying the free-surface profile along the jump reach, producing a longitudinal water-surface trace that captures the rise, oscillations, and gradual stabilization downstream. Tailwater control was provided by a downstream gate/valve, and its opening ratio was noted for each run because it directly regulates tailwater depth and, consequently, the jump type, location, and degree of submergence .In selected tests, the investigation was extended beyond integral depths and lengths by measuring the vertical velocity profile at chosen sections within the jump. These velocity data help reveal how the distribution of streamwise velocity evolves through the roller, providing insight into turbulence intensity, momentum exchange, and mixing processes that cannot be inferred from depth measurements alone. After the experiments, all recorded variables were post-processed to compute derived quantities appropriate to the study objectives—typically including hydraulic-jump characterization and performance metrics such as Froude numbers, sequent-depth ratios, relative energy loss, momentum (conjugate-depth) consistency checks, normalized jump and roller lengths, and other non-dimensional indicators used to compare runs and assess the effect of boundary conditions or basin geometry.

- **Froude number upstream of the jump, Fr1** (based on y1and the corresponding mean velocity).
- **Sequent depth ratio, y2/y1** and/or **relative jump height (y2−y1)/y1(y_2-y_1)**.
- **Energy loss across the jump** (difference in specific energy before and after the jump) and **energy dissipation efficiency**.
- **Relative jump length** Lj/y1 or Lj/(y2−y1) and **relative roller length**.
- Any additional non-dimensional parameters relevant to the roughness configuration and tailwater control (e.g., relationships involving TW gate opening).

$\left({Lj}/{y_2} \right)$ و $\left({y_2}/{y_1} \right)$ ، (Fr)in order to realize the results, 60 experiments have been conducted by the researcher.

For each dimension of bed roughness, 5 discharges and 5 Froud numbers s (1.4 >Fr >10.99) and four positive slopes of 0, 0.1, 0.2 and 0.3 were tested.

- **Discussion & conclusion:**
- **Comparison of secondary to primary depth ratio and jump length to secondary depth ratio at zero slope**

In this division, in figures 2-a, 2-b and 2-c, changes in the ratio of secondary to primary depth and changes in jump length to secondary depth have been plotted against the corresponding primary landing number at zero percent slope in bed roughness.

Civil and Project Journal, 2026, 8(8), 51-81
https://doi.org/10.22034/cpj.2026.585612.1448

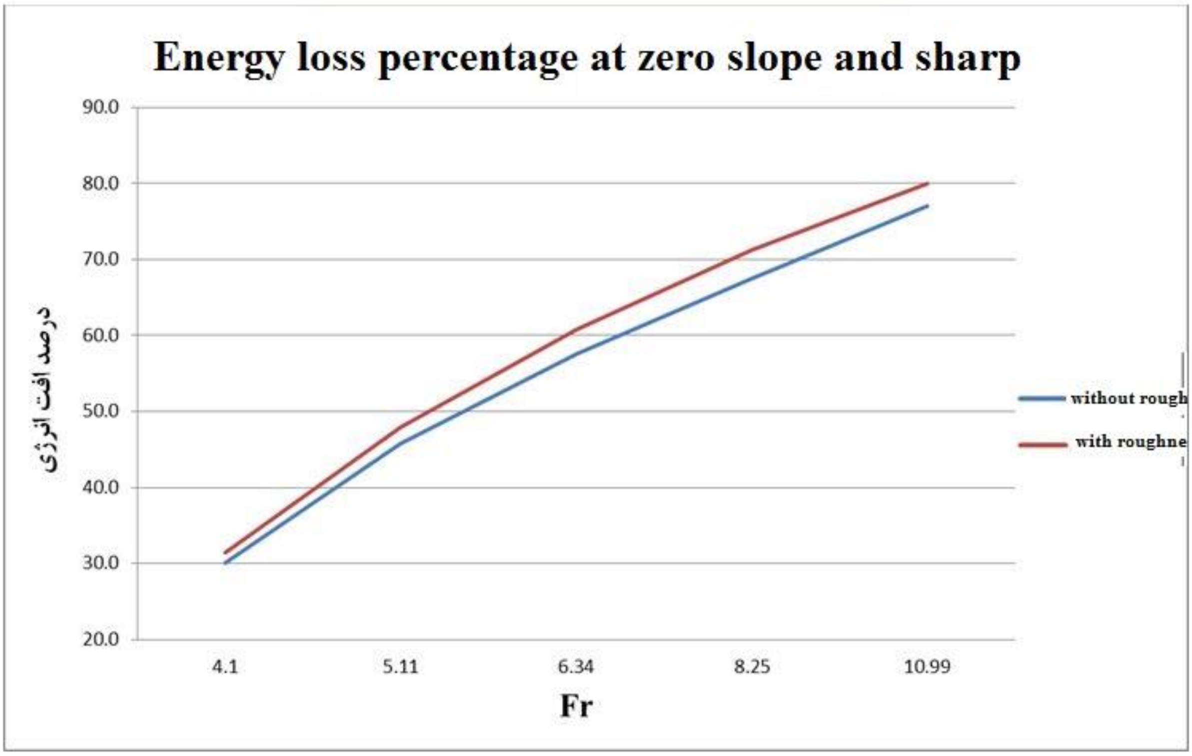

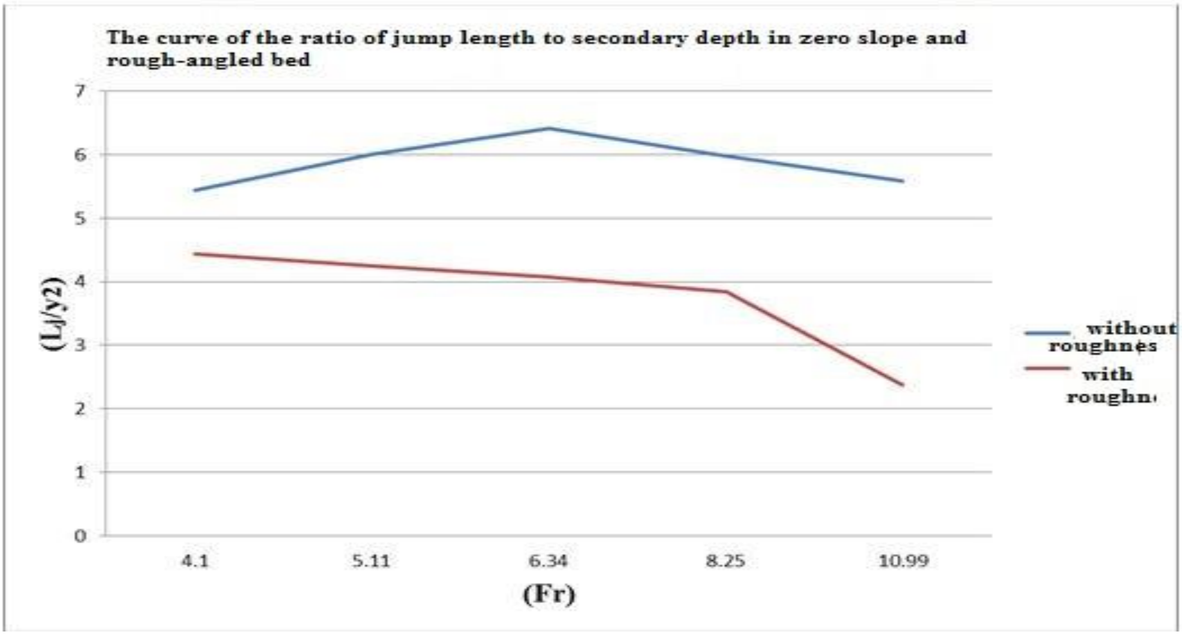

A: Ratio diagram y2/y1

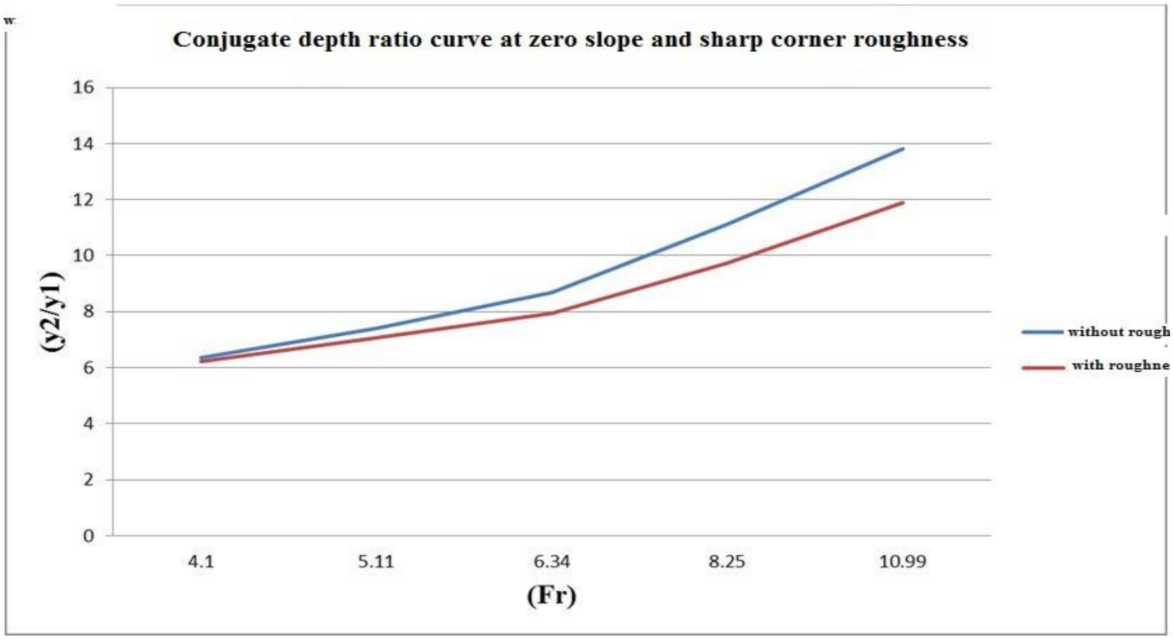

b) graph of $\frac{L_j}{y_2}$

c) Graph of energy loss percentage Fr

Figure 9: Test results at zero percent slope and rhombic roughness

The experimental results indicate that the installation of **rhombic roughness elements** produces a measurable improvement in hydraulic-jump performance compared with the smooth-bed condition. Overall, the **conjugate (sequent) depth** shows a **9.6% reduction** (reported to one decimal place) when rhombic roughness is used. This reduction is practically important because a smaller conjugate depth means the required tailwater depth downstream of energy dissipators can be reduced, which can help decrease excavation depth, sidewall height, and construction cost in stilling basins. A more pronounced effect is observed on the hydraulic-jump extent. The ratio of jump length to secondary **depth**, Lj/y2decreases by **35.5%** (one-decimal precision) in the presence of rhombic roughness. This suggests that the roughness accelerates the stabilization of the flow and shortens the region over which intense turbulence and roller action persist. In design terms, this behavior is desirable because it implies that the stilling basin length required to contain the jump can be significantly reduced, provided that the jump remains stable and does not sweep out under the same tailwater conditions. Energy dissipation results are consistent with these trends. The **percentage energy loss** across the hydraulic jump is reported as **5**5.6% for the smooth bed **and** 58.3% for the rhombic-roughened bed. Although the numerical increase (about 2.7 percentage points) may appear modest, it indicates a clear enhancement in dissipative capacity. Physically, rhombic roughness promotes additional turbulence production near the bed, increases form drag, strengthens mixing within the roller, and thereby converts a larger fraction of the incoming kinetic energy into turbulence and heat. Regarding the conjugate-depth ratio, the study shows that for the rhombic-roughness case, y2/y1 **increases as the upstream Froude number increases**. This is expected hydraulic-jump behavior: as the incoming flow becomes more supercritical (higher Fr1), the jump becomes stronger and requires a larger downstream depth to satisfy momentum balance. However, when comparing smooth and rough beds at the **same Froude number**, the data indicate that y2/y1**is smaller with rhombic roughness**. This implies that roughness modifies the momentum exchange and shear stresses in such a way that the flow transitions to subcritical conditions at a relatively lower sequent depth than would be required on a smooth bed.A similar comparative outcome is reported for the relative jump length. For a given Froude number, the ratio Lj/y2 is **reduced** by installing rhombic roughness. Mechanistically, the roughness elements intensify near-bed turbulence and enhance momentum diffusion in the lower part of the flow. This increases the rate at which the incoming supercritical jet loses coherence and mixes with the surrounding water, causing the roller to develop and decay over a shorter distance. In practice, a shorter Lj for comparable flow conditions is advantageous because it can reduce the risk of downstream scour and lessen the spatial footprint of the energy dissipation structure.

Finally, the overall discussion points to a consistent conclusion: rhombic roughness increases energy loss and simultaneously reduces both conjugate depth and relative jump length at equal upstream Froude number. These combined effects indicate improved energy dissipation efficiency and more compact jump formation, which are both favorable for hydraulic-structure design. At the same time, it is important to interpret these findings within the tested range of discharges, Froude numbers, and roughness geometry; roughness performance can depend on factors such as relative submergence k/y1roughness spacing/density, and tailwater control. For design application, the reported reductions (9.6% in conjugate depth and 35.5% in Lj/y2along with increased energy loss) strongly support the use of rhombic roughness as an effective bed treatment for enhancing hydraulic-jump control and reducing stilling-basin dimensions.

- **Comparison of secondary to primary depth ratio and jump length to secondary depth ratio in 0.1% slope**

In this part, in figures 3-a, 3-b and 3-c, the changes in the secondary to primary depth ratio and the changes in the jump length to the secondary depth against the corresponding primary descent number in the slope of 0.1% are specified in the roughness of the rhombus of the bed.

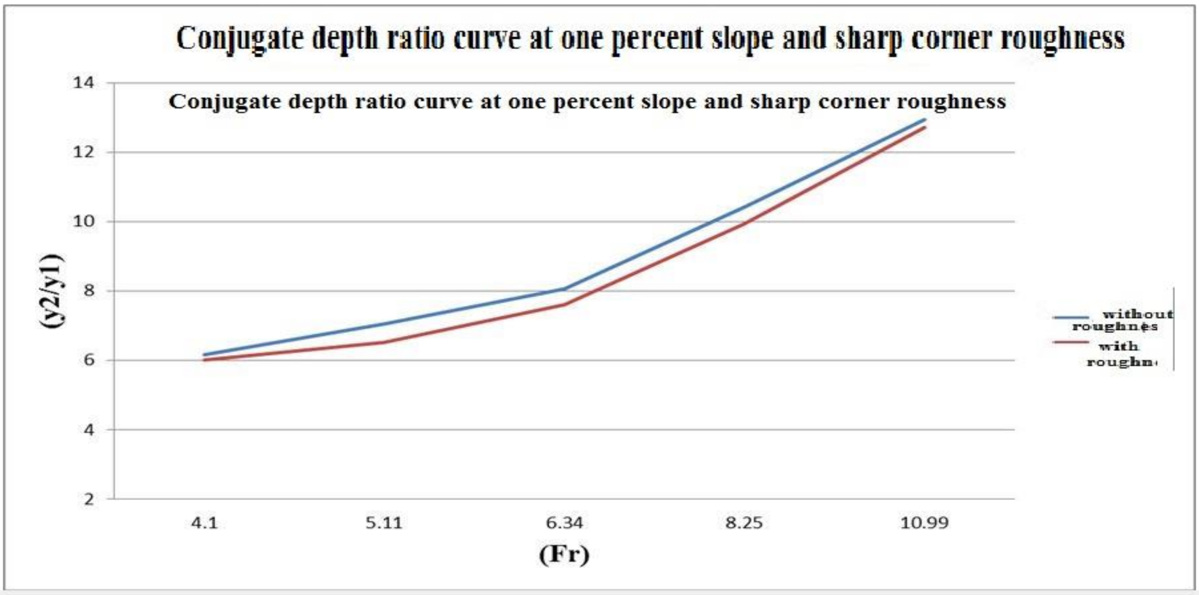

a) graph related to ration of $\frac{y_2}{y_1}$

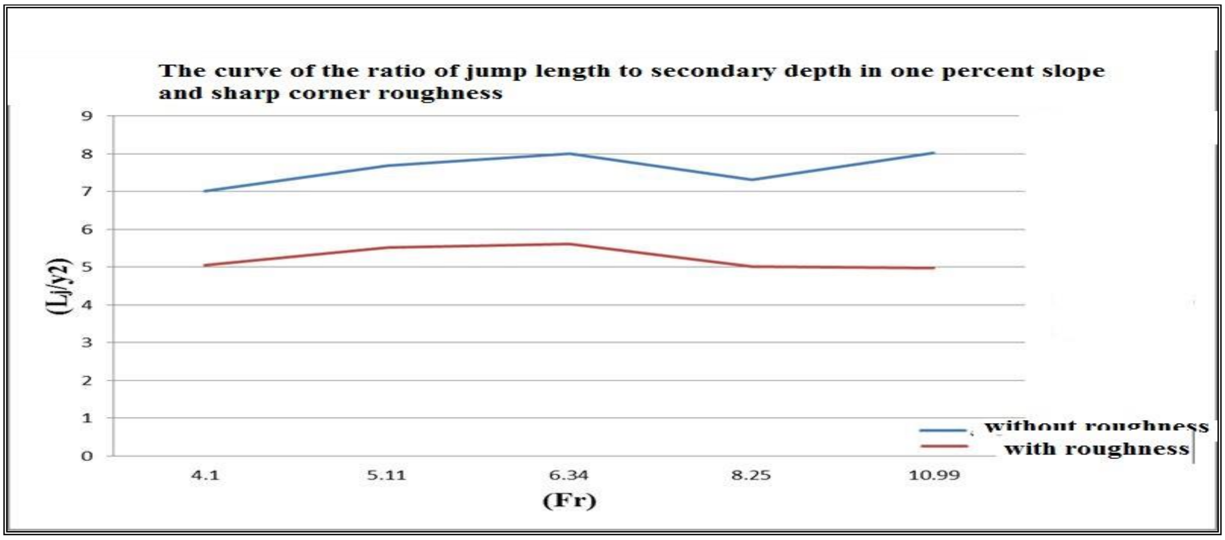

b) Graph related to ratio of $\frac{L_j}{y_2}$

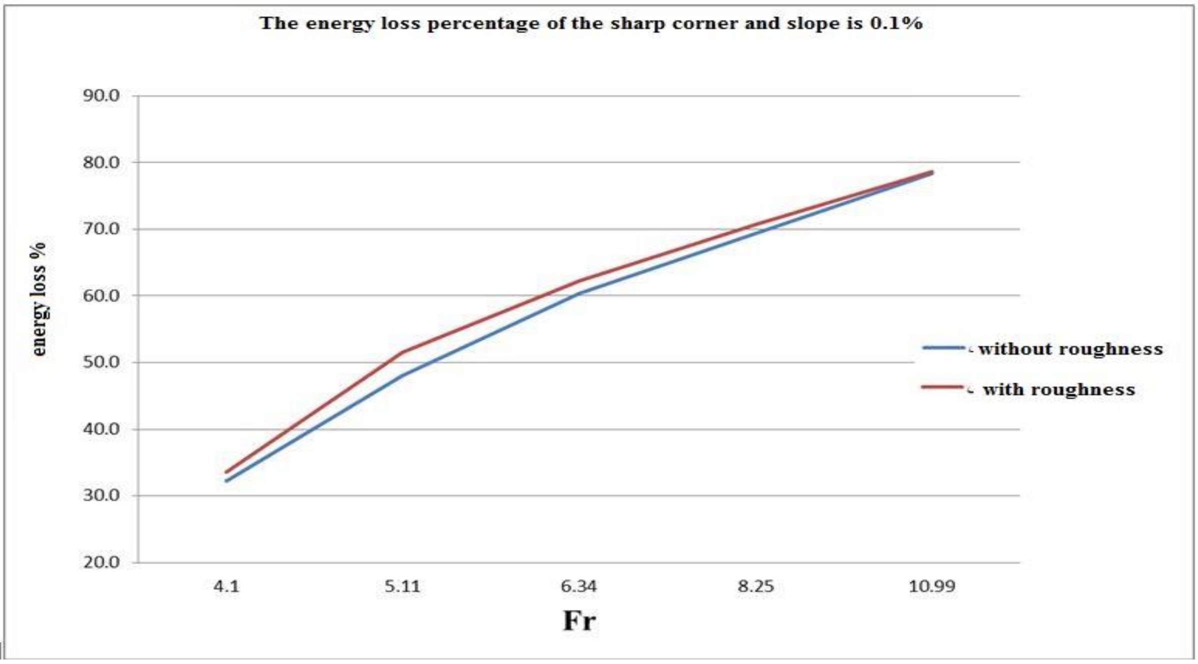

c) Graph of energy loss percentage to Fr

Figure 10: Test results at 0.1% slope and rhombic roughness

At a channel bed slope of 0.1%, the experimental findings confirm that installing rhombic roughness elements still improves hydraulic-jump performance compared with the smooth-bed condition, although the magnitude of some effects is smaller than in the zero-slope case. The data show that the conjugate (sequent) depth is reduced by 4.1% (rounded to one decimal place) when rhombic roughness is used. This reduction indicates that, for the same inflow conditions, the downstream depth required to maintain a stable jump becomes slightly lower, which can be beneficial in practical stilling-basin design by reducing required tailwater depth and potentially lowering wall height or excavation needs. A stronger influence is observed on the longitudinal development of the jump. The ratio of hydraulic jump length to secondary depth, Lj/y2decreases by 31.2% (one-decimal precision) under rhombic roughness. This result suggests that roughness substantially shortens the region over which the roller and intense turbulence persist. From a hydraulic-engineering standpoint, a smaller Lj/y2implies that the jump can be contained in a shorter basin length, which is important for limiting construction cost and minimizing downstream scour risk—provided that the jump remains stable and the toe position is controllable. The measurements of energy dissipation are consistent with these geometric changes. The energy loss percentage across the jump is reported as 57.7% for the smooth bed and 59.3% for the rhombic-roughened bed. While the increase is not extremely large in absolute terms (about 1.6 percentage points), it demonstrates a clear trend: rhombic roughness enhances the conversion of incoming kinetic energy into turbulence and heat. Physically, this occurs because roughness elements introduce additional form drag, increase near-bed turbulence production, and intensify mixing within the roller—thereby increasing overall dissipation even when the channel has a mild slope. With respect to the depth ratio, the results show that for the rhombic-roughness configuration, y2/y1increases with increasing upstream Froude number. This is expected behavior for hydraulic jumps: higher Fr1Fr_1Fr1 represents stronger supercritical flow, so a larger sequent depth is required for the downstream flow to satisfy momentum balance. However, when the smooth and rough cases are compared at the same Froude number, the study indicates that y2/y1becomes smaller with rhombic roughness. In other words, for equivalent inflow intensity, the roughened bed enables the jump to reach subcritical conditions with a slightly smaller conjugate depth, reflecting enhanced momentum exchange and shear effects introduced by the roughness.A similar comparison applies to the length ratio. For a given Froude number, installing rhombic roughness leads to a reduction in Lj/y2 . This can be interpreted as a consequence of faster momentum diffusion and stronger turbulence generation near the bed, which breaks down the supercritical jet more rapidly and reduces the distance needed for the roller to decay and for the free surface to become relatively stable. In practical terms, this is one of the most valuable outcomes of roughness: even if the reduction in conjugate depth is moderate at 0.1% slope, the reduction in relative jump length remains large, indicating a more compact and efficient stilling process. Overall, the slope of 0.1% does not change the qualitative conclusions: rhombic roughness increases energy loss and decreases both y2/y1 and Lj/y2at a fixed Froude number. The smaller reduction in conjugate depth (4.1%) compared with typical horizontal-bed improvements can be attributed to the fact that a mild slope affects tailwater control and the pressure distribution along the jump, potentially making the sequent depth less sensitive to bed treatments than the jump length is. Nevertheless, the combined evidence—higher dissipation (59.3% vs. 57.7%) and substantially shorter relative jump length (31.2% decrease)—supports the conclusion that rhombic roughness remains an effective method for improving hydraulic-jump energy dissipation and reducing stilling-basin length under slightly sloping-bed conditions. If you want, I can rewrite this as a polished "Results and Discussion" subsection (more formal, journal style) and explicitly connect the trends to hydraulic-jump theory (momentum equation, relative submergence k/y1and slope effects).

.

Comparison of secondary to primary depth ratio and jump length to secondary depth ratio in 0.2% slope

In this section, in figures 4-a, 4-b and 4-c, the changes in the secondary to primary depth ratio and the changes in the jump length to the secondary depth are shown in the rhombus roughness of the bed in contrast to the corresponding primary descent number in the slope of 0.2%..

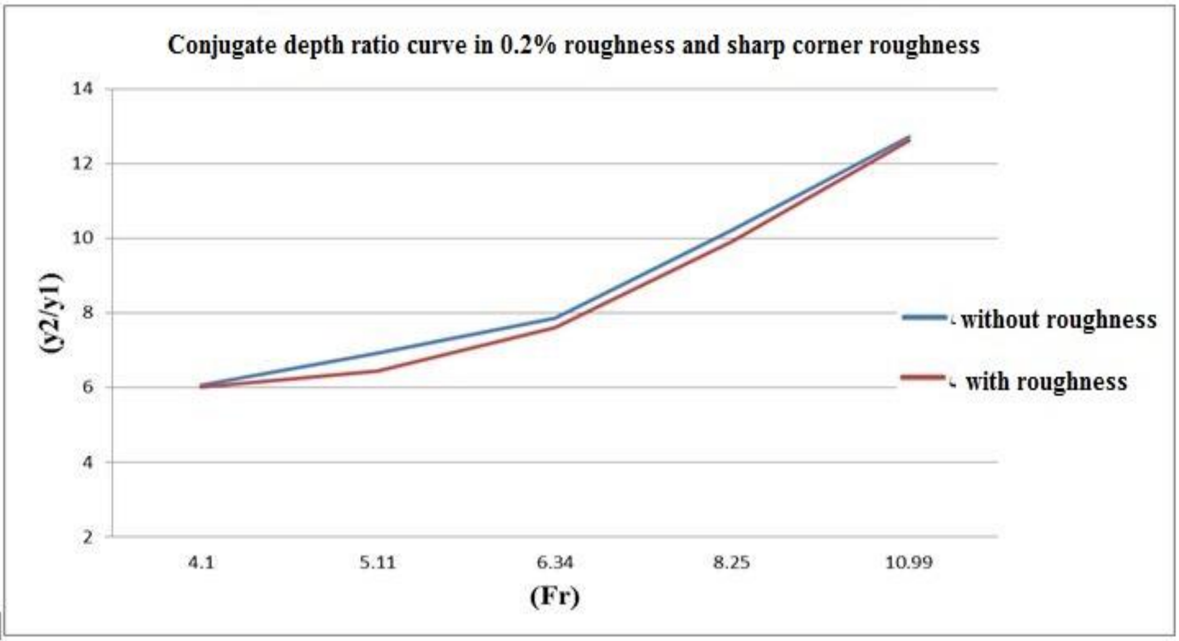

A) ratio diagram $\frac{y_2}{y_1}$

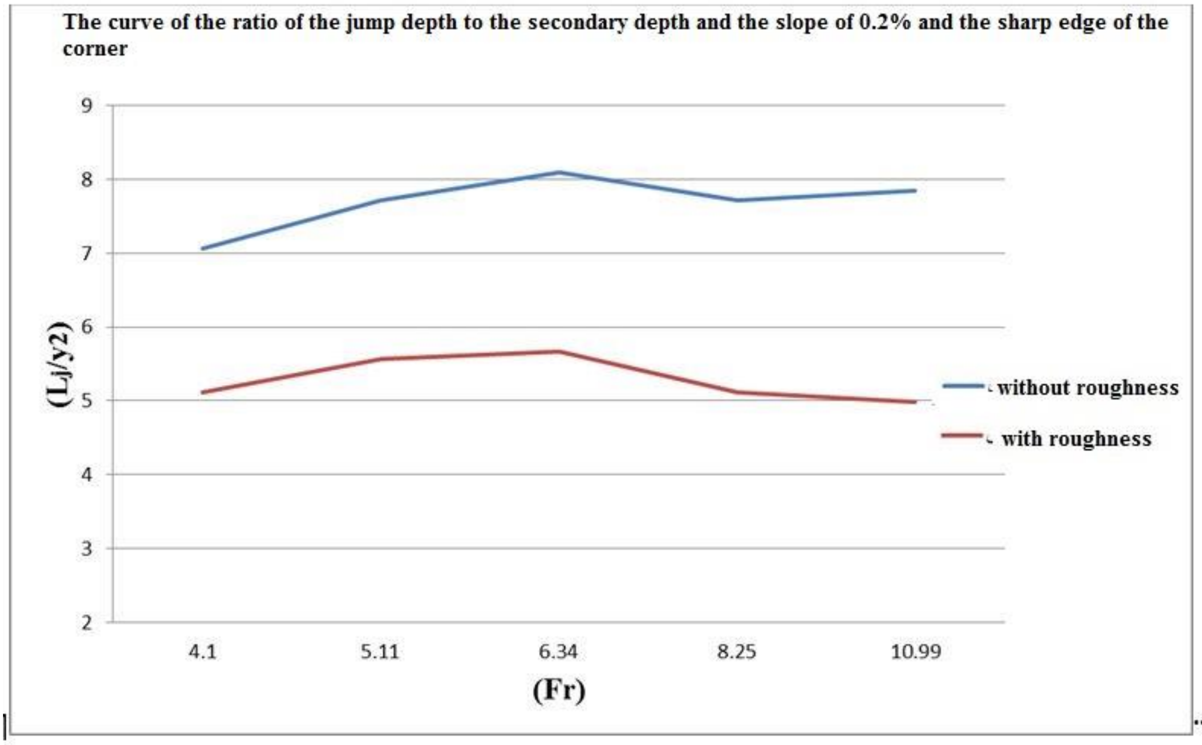

b) ratio diagram $\frac{L_j}{y_2}$

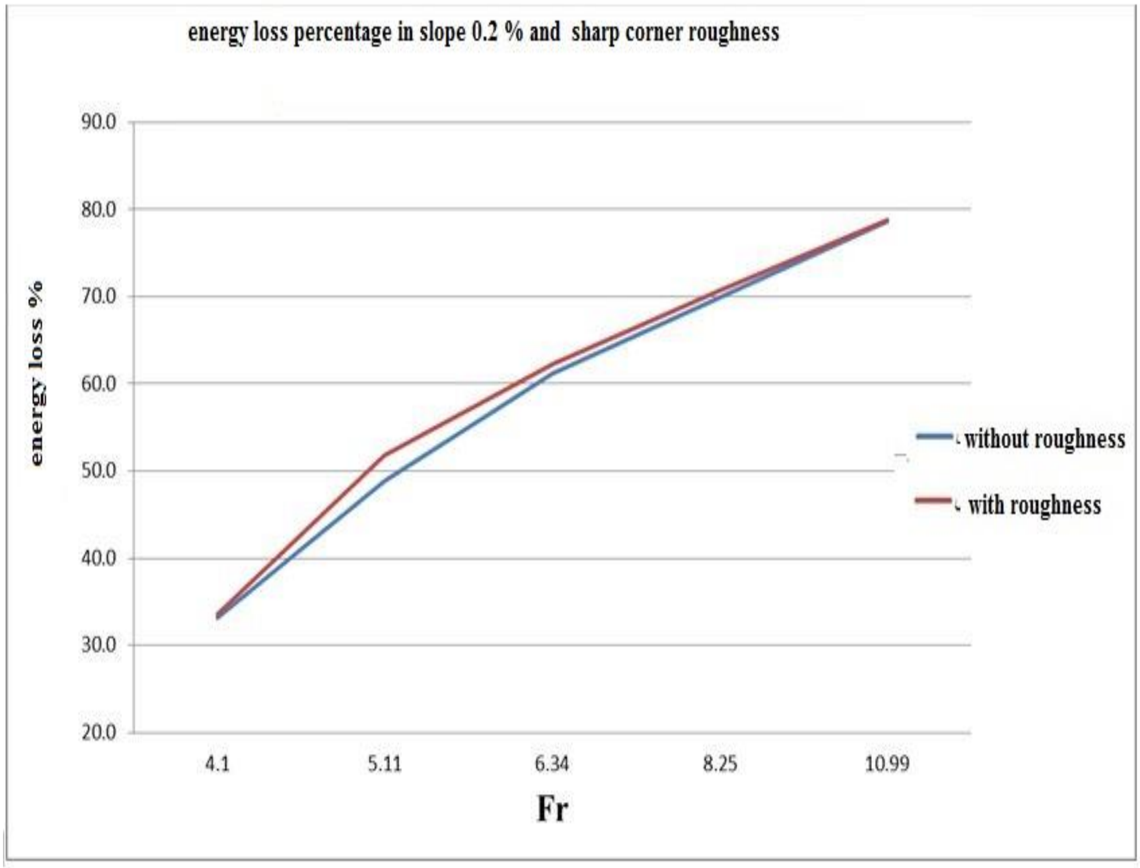

c) Graph of energy loss percentage to Fr

Figure 11: Test results in 0.2% slope and rhombic roughness

The experiments show that, at a bed slope of **0.2%**, installing rhombic roughness leads to a measurable reduction in key hydraulic-jump characteristics compared with a smooth bed. Specifically, the **conjugate (sequent) depth** is reduced by **2.65%** (reported with one-decimal precision in the study), indicating that the downstream depth required to form the jump becomes slightly smaller when roughness elements are present. A much stronger effect is observed in the jump development length. The results indicate that rhombic roughness decreases the **ratio of** jump length to secondary depth (Lj/y2by **31.2%**, meaning the hydraulic jump becomes considerably more compact. This implies that the roller region and associated turbulence decay over a shorter distance, which is beneficial for practical design because it can reduce the required stilling-basin length or help confine the jump within an existing basin footprint. In terms of energy dissipation, the average **percentage of energy reduction (energy loss)** is **58.4%** for the **smooth bed** and **59.5%** for the bed with **rhombic roughness**. Although the increase in energy loss due to roughness is modest in magnitude (about **1.1 percentage points** on average), it confirms that rhombic elements enhance turbulence production and form drag, thereby extracting slightly more energy from the supercritical inflow.

The dimensionless trends also remain consistent with hydraulic-jump physics. For the rhombic-roughened bed, the depth ratio (y2/y1) **increases with increasing Froude number**, reflecting stronger jumps at higher approach flow intensity. However, for a **given Froude number**, the installation of rhombic roughness **reduces** (y2/y1) relative to the smooth-bed case. Likewise, for a given inflow condition, (Lj/y2) **decreases** with rhombic roughness, while the **percentage of energy loss increases**, demonstrating that roughness promotes faster dissipation and shorter jump development.

Table 11 Summary of the effect of rhombic roughness on hydraulic-jump characteristics (slope = 0.2%)

Parameter / Indicator	Smooth bed	Rhombic roughness	Reported effect of rhombic roughness
Conjugate depth reduction	—	—	**2.65% decrease** in conjugate depth
Decrease in Lj/y2	—	—	**31.2% decrease**
Average energy reduction (energy loss)	**58.4%**	**59.5%**	**Increase** in energy loss (≈ **+1.1** percentage points)
Trend of y2/y1with Fr	Increases with Fr	Increases with Fr	Same overall trend; **lower** y2/y1for a given Fr with roughness
Trend of Lj/y2 for a given inflow	Baseline	Smaller	**Decreases** with roughness

Table 1 compiles the main quantitative and qualitative outcomes comparing smooth and rhombic-roughened beds at a 0.2% slope. The rhombic roughness produces a small but clear reduction in conjugate depth (2.65%) and a large reduction in normalized jump length (31.2%), indicating a more compact jump. Energy dissipation also increases slightly (58.4% to 59.5%), supporting the conclusion that roughness enhances turbulence and form drag. Finally, the dimensionless behavior shows that although (y2/y1) rises with Froude number as expected, rhombic roughness lowers (y2/y1and (Lj/y2) for a given inflow condition, while increasing the overall energy loss.

Comparison of secondary to primary depth ratio and jump length to secondary depth ratio in 0.3% slope.

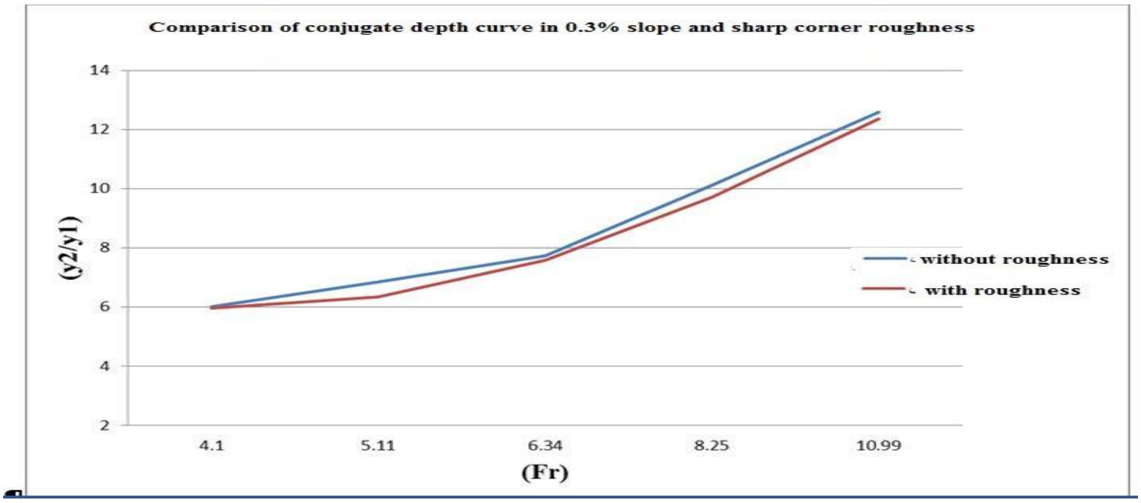

A) Ratio diagram $\frac{y_2}{y_1}$

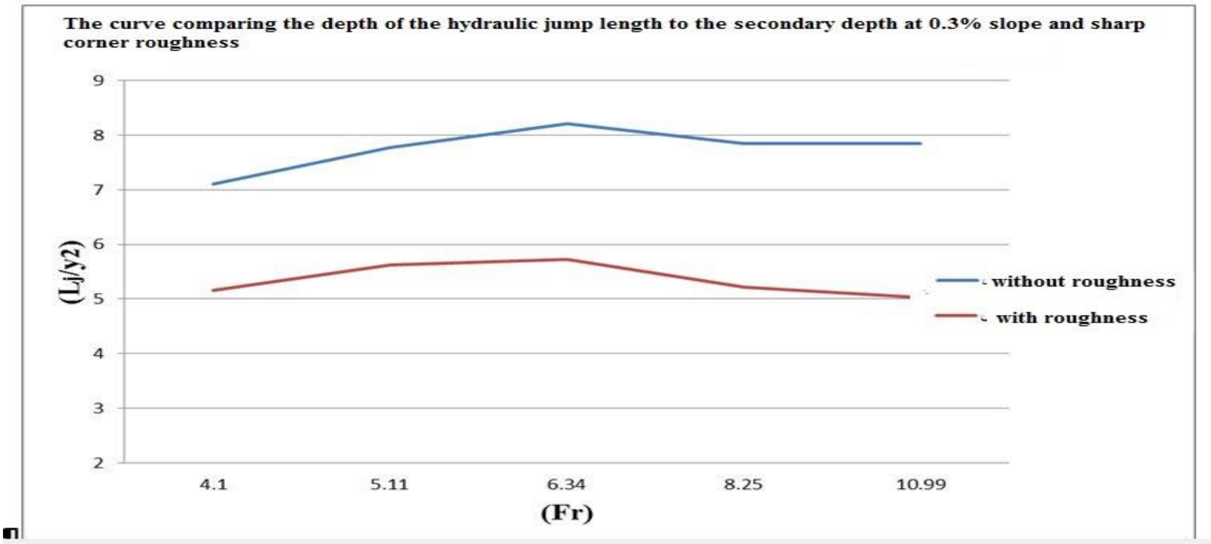

b) ratio diagram $\frac{L_j}{y_2}$

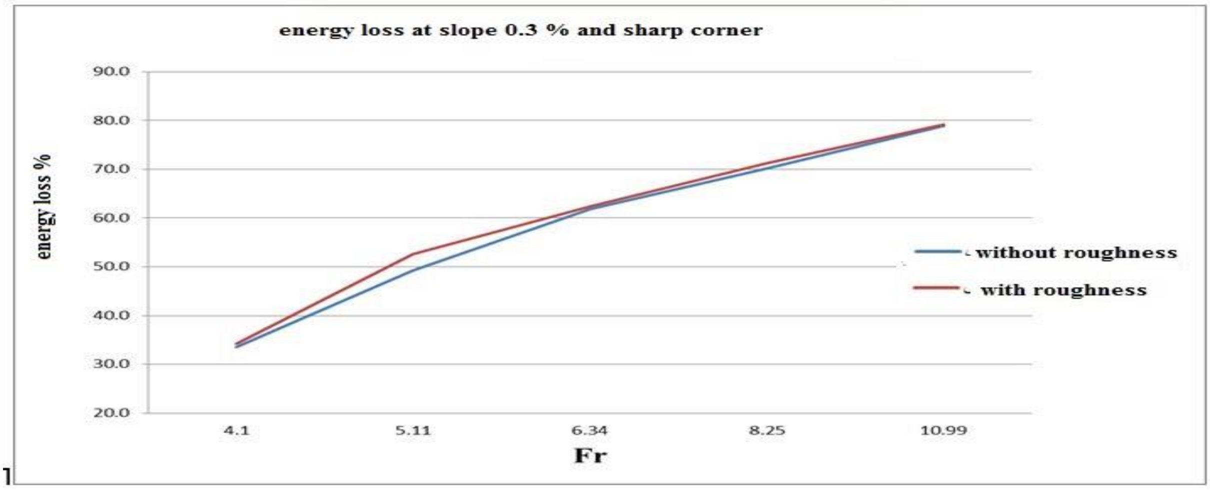

c) Graph of energy loss percentage to Fr

Figure 12: Test results in 0.3% slope and rhombic roughness

Figure 5 shows that increasing the channel bed slope to **0.3%** and adding **rhombic (diamond-shaped) roughness elements** leads to noticeable changes in the hydraulic-jump characteristics compared with a smooth bed. The results indicate that the hydraulic jump becomes more compact and hydraulically more efficient when these roughness elements are present. In particular, both the downstream flow depth and the jump length are affected, while the overall dissipation of flow energy is slightly improved. These changes suggest that bed roughness does not merely disturb the flow locally, but significantly modifies the turbulence structure and momentum exchange within the jump region.

One of the observed effects is a reduction in the **conjugate or sequent depth**. At the 0.3% slope, the sequent depth decreases by **3.16%** in the presence of rhombic roughness. Although this reduction is relatively small, it is still hydraulically meaningful because it indicates that the downstream depth required for jump formation becomes slightly smaller than in the smooth-bed case. This behavior can be attributed to the additional resistance and turbulence generated by the roughness elements near the channel bed. In other words, the rhombic projections help redistribute momentum and promote stronger mixing, which slightly lowers the final downstream depth needed to satisfy the hydraulic-jump conditions.

A much stronger effect is seen in the **jump length**. The data show that the normalized jump length, is reduced by **31.1%** when rhombic roughness is installed. This is a significant reduction and indicates that the hydraulic jump develops and stabilizes over a much shorter distance. From an engineering perspective, this is highly beneficial because a shorter jump can reduce the required length of a stilling basin and improve the ability of the basin to contain the jump effectively. Such a reduction can contribute to more economical and efficient hydraulic-structure design, especially where space or construction cost is an important consideration.

The energy dissipation results support the same conclusion. The average energy loss increases from **58.7%** for the smooth bed to **60.0%** for the rhombic roughness case, showing an improvement of about **1.3 percentage points**. This increase suggests that the roughness elements enhance energy dissipation by creating additional form drag, flow separation, and turbulence production. Furthermore, the dimensionless relationships remain consistent with hydraulic-jump theory: the depth ratio increases as the Froude number increases, but for the same Froude number it is slightly lower under rhombic roughness than under smooth-bed conditions. Likewise, the relative jump length is also smaller with roughness. Overall, the findings confirm that rhombic roughness at a 0.3% bed slope improves hydraulic-jump performance by producing a shorter, more stable, and slightly more energy-dissipative jump.

Conclusion:

Hydraulic jumps dissipate a substantial portion of a flow’s kinetic energy by transforming it into turbulence, intense mixing, air entrainment, and heat. For this reason, energy-dissipation structures such as stilling basins located downstream of spillways, weirs, sluice gates, and diversion dams are commonly designed to force the hydraulic jump to occur within a protected reach. By confining the jump to a controlled zone, engineers can significantly reduce bed erosion, structural scour, and downstream damage. The hydraulic jump therefore remains one of the most important natural mechanisms used in hydraulic engineering for safely converting supercritical flow into subcritical flow while simultaneously dissipating excess energy.

Based on the findings of the present research, rhombic (diamond-shaped) bed roughness measurably alters the characteristics of the classical hydraulic jump. In comparison with a conventional jump forming over a smooth or flat bed, the presence of rhombic roughness reduced the conjugate, or sequent, depth by approximately **2.65% to 9.6%**, with an average reduction of **6.13%**. From a practical engineering perspective, this result suggests that under similar inflow conditions, the downstream tailwater depth required to establish and sustain the jump can be somewhat lower when rhombic roughness is provided. This can be particularly advantageous in field situations where the available tailwater depth is limited, where excavation depth must be minimized, or where a more economical basin geometry is desired. An even more significant improvement was observed in the hydraulic jump length. Relative to the classical jump on a smooth bed, rhombic roughness reduced the normalized jump length, Lj/y2 by approximately **35.5%**. This finding is especially important for the design and optimization of stilling basins, because it indicates that the jump becomes more compact and that the roller region shortens considerably. In engineering terms, this can lead to a reduction in the required basin length or can improve the ability to contain the jump within an existing structure. Such a reduction in jump length is often highly desirable because basin length is directly related to construction cost, space limitations, and the overall feasibility of hydraulic energy dissipators in real projects.

From a physical standpoint, the improved performance associated with rhombic roughness can be attributed to several interacting flow mechanisms. The roughness elements increase near-bed turbulence intensity, generate local flow separation, create additional form drag, and enhance three-dimensional mixing throughout the roller region. These processes accelerate the decay of the incoming supercritical jet and promote a faster redistribution of momentum between the upper and lower layers of the flow. As a result, the flow transitions more rapidly toward the downstream subcritical regime, thereby shortening the distance required for stabilization. In other words, the roughened bed does not simply resist the flow; rather, it actively modifies the internal structure of the jump in a way that promotes more efficient energy dissipation over a shorter distance.The dimensionless relationships with Froude number further support this interpretation. For the rhombic-roughened bed, increasing the Froude number caused the depth ratio, y2/y1 y_2 / y_1 y2/y1, to increase by about **6.5% on average**, which is consistent with the well-established behavior of hydraulic jumps: stronger incoming supercritical flow produces a stronger jump and therefore a larger sequent-depth ratio. However, when roughened and smooth-bed cases were compared at the same Froude number, the rhombic roughness produced a slight decrease in the normalized jump length, Lj/y2 of about **1.2% on average**, along with a reduction in the depth ratio, y2/y1 of up to **2%**. This combined behavior indicates that the roughness does more than increase resistance in a conventional sense. Instead, it changes how momentum and turbulence are distributed within the jump, allowing post-jump flow conditions to be achieved with a slightly smaller relative depth and over a reduced distance. The energy-loss analysis also confirms the overall benefit of using rhombic roughness. The results show that the percentage of energy loss increased by approximately **1.7% on average** when rhombic roughness was installed. Although this increase may appear modest when compared with the much larger reduction in jump length, it is hydraulically meaningful because energy dissipation in hydraulic jumps is already naturally high. Therefore, even a small additional increase in energy loss indicates a significant modification of turbulence structure and dissipation mechanisms. The roughness likely enhances this process by increasing turbulence production near the bed, strengthening recirculation, and promoting greater air entrainment and fluid mixing. These effects help explain why the hydraulic jump becomes shorter, more controlled, and potentially more stable when formed over a rhombic-roughened surface. Overall, the results demonstrate that rhombic bed roughness can improve stilling basin performance in several important ways. Its primary benefit appears to be the substantial compression of jump length, which offers strong practical value for basin design. At the same time, it slightly reduces sequent depth and produces a small but consistent increase in energy dissipation. Taken together, these outcomes indicate that rhombic roughness is a promising modification for enhancing the hydraulic efficiency of stilling basins, especially where compact design, reduced tailwater requirement, and improved flow containment are important considerations. In addition, the reduction in conjugate depth and jump length suggests that rhombic roughness may contribute to more economical hydraulic structures. A shorter stilling basin can reduce excavation, concrete volume, reinforcement requirements, and overall construction cost. Likewise, a slightly lower required tailwater depth may provide greater design flexibility in channels or outlets where downstream water levels cannot always be guaranteed. These practical implications are highly relevant in water-resources engineering, particularly in arid and semi-arid regions or in retrofit projects where space and budget constraints are major concerns. Therefore, the observed hydraulic improvements are not only of theoretical interest but also of direct significance to real-world design. Another important aspect of these findings is their contribution to the broader understanding of rough-bed hydraulic jumps. While many previous studies have shown that artificial roughness can modify jump behavior, the present results indicate that rhombic roughness offers a favorable balance between geometric simplicity and hydraulic effectiveness. The diamond-shaped elements appear to interact efficiently with the high-velocity incoming flow, producing enhanced turbulence and momentum exchange without causing undesirable flow conditions. This suggests that the geometry of roughness elements is an important design parameter and that not all roughness configurations produce the same hydraulic response. Consequently, rhombic roughness may be considered a useful alternative to more traditional roughening arrangements in the design of energy-dissipation systems. Finally, although the present findings are promising, they also highlight the need for further investigation. Future studies could examine the influence of rhombic roughness size, spacing, orientation, and relative height under a wider range of Froude numbers and flow conditions. It would also be valuable to assess the performance of this roughness under sediment-laden flow, fluctuating tailwater conditions, and prototype-scale applications. Numerical modeling and detailed velocity measurements could further clarify the internal turbulence structure and help explain the precise mechanisms responsible for the observed reductions in sequent depth and jump length. Such future work would strengthen the basis for developing design recommendations and support the integration of rhombic roughness into practical stilling basin engineering.

Refrences

1. Abbaspour, A., Hosseinzadeh Dalir, A., Farsadizadeh, D., & Sadraddini, A. A. (2019). Effect of screens on the characteristics of hydraulic jump in a rectangular channel. Journal of Irrigation and Drainage Engineering, 145(7), 04019012. https://doi.org/10.1061/(ASCE)IR.1943-4774.0001459
2. Ali, C. Z., & Kaleem, S. M. (2015). Launching/disappearance of stone apron, block floor downstream of the Taunsa Barrage and unprecedented drift of the river towards Kot Addu Town. Science and Technology Development, 34, 60–65. https://doi.org/10.3923/std.2015.60.65
3. Aydogdu, M., Gul, E., & Dursun, O. F. (2022). Experimentally verified numerical investigation of the sill hydraulics for abruptly expanding stilling basin. Arabian Journal for Science and Engineering. https://doi.org/10.1007/s13369-022-07089-6
4. Babaali, H., Shamsai, A., & Vosoughifar, H. (2015). Computational modeling of the hydraulic jump in the stilling basin with convergence walls using CFD codes. Arabian Journal for Science and Engineering, 40, 381–395. https://doi.org/10.1007/s13369-014-1466-z
5. Bakhmeteff, B. A., & Matzke, A. E. (1936). The hydraulic jump in terms of dynamic similarity. Transactions of the ASCE, 100, 630–680.
6. Balkiş, A. (2004). Effect of screen inclination on energy dissipation downstream of hydraulic structures. Journal of Hydraulic Engineering, 130(6), 610–614.
7. Bantacut, A. Y., Azmeri, A., Jemi, F. Z., Ziana, Z., & Muslem, M. (2022). An experiment of energy dissipation on USBR IV stilling basin—Alternative in modification. Journal of Water and Land Development, 53, 68–72. https://doi.org/10.24425/jwld.2022.140781
8. Bayon-Barrachina, A., & Lopez-Jimenez, P. A. (2015). Numerical analysis of hydraulic jumps using OpenFOAM. Journal of Hydro informatics, 17, 662–678. https://doi.org/10.2166/hydro.2015.041
9. Bélanger, J. B. (1841). Notes sur l'hydraulique. École Royale des Ponts et Chaussées.
10. Behrouzi-Rad, R., Hosseinzadeh Dalir, A., Farsadizadeh, D., & Salmasi, F. (2013). Experimental study of the effect of perforated sills on the characteristics of a forced hydraulic jump. Journal of Civil Engineering and Urbanism, 3(4), 146–152.
11. Bhosekar, V. V., Patnaik, S., Gadge, P. P., & Gupta, I. D. (2014). Discharge characteristics of orifice spillway. International Journal of Dam Engineering, 5–18. [missing volume/issue/pages formatting as per journal]
12. Bozkuş, M., & Aslankara, G. (2008). Influence of tailwater depth and multiple permeable screens on hydraulic jump energy dissipation. Journal of Hydraulic Research, 46(4), 520–530.
13. Bozkuş, M., Aslankara, G., & Karahan, S. (2008). Energy dissipation of hydraulic jumps using permeable screens: Effects of porosity, thickness, and screen location. Journal of Hydraulic Engineering, 134(11), 1676–1681.

14. Bremen, R., & Hager, W. H. (1994). Expanding stilling basin. Proceedings of the Institution of Civil Engineers: Water, Maritime and Energy, 106(3), 215–228.

15. Carvalho, R. F., Lemos, C. M., & Ramos, C. M. (2008). Numerical computation of the flow in hydraulic jump stilling basins. Journal of Hydraulic Research, 46, 739–752. https://doi.org/10.1080/00221686.2008.9521919

16. Chachereau, Y., & Chanson, H. (2011). Free-surface fluctuations and turbulence in hydraulic jumps. Experimental Thermal and Fluid Science, 35, 896–909. https://doi.org/10.1016/j.expthermflusci.2011.01.009

17. Chanson, H., & Gualtieri, C. (2008). Similitude and scale effects of air entrainment in hydraulic jumps. Journal of Hydraulic Research, 46, 35–44. https://doi.org/10.1080/00221686.2008.9521841

18. Chaudhry, Z. A. (2010a). Performance assessment of Taunsa Barrage subsidiary weir for long term rehabilitation planning. Pakistan Journal of Engineering and Applied Sciences, 7, 65–70.

19. Chaudhry, Z. A. (2010b). Surface flow hydraulics of Taunsa Barrage: Before and after rehabilitation. [missing source (journal/proceedings), volume, pages]

20. Chaudhary, Z. A., & Sarwar, M. K. (2014). Rehabilitated Taunsa Barrage: Prospects and concerns. Science and Technology Development, 33, 127–131.

21. Daneshfaraz, R., Sadeghfam, S., & Ghahramanzadeh, A. (2017). Three-dimensional numerical investigation of flow through screens as energy dissipators. Canadian Journal of Civil Engineering, 44(10), 850–859. https://doi.org/10.1139/cjce-2017-0273

22. Gadge, P. P., Jothiprakash, V., & Bhosekar, V. V. (2018). Hydraulic investigation and design of roof profile of an orifice spillway using experimental and numerical models. Journal of Applied Water Engineering and Research, 6, 85–94. https://doi.org/10.1080/23249676.2016.1214627

23. Hager, W. H., & Bremen, R. (1989). Classical hydraulic jump: Sequent depths. Journal of Hydraulic Research, 27, 565–585. https://doi.org/10.1080/00221688909499111

24. Hager, W. H., & Li, D. (1992). Sill-controlled energy dissipator. Journal of Hydraulic Research, 30, 181–[missing end page]. https://doi.org/10.1080/00221689209498932

25. Hirt, C. M., & Sicilian, J. M. (1985). A porosity technique for the definition of obstacles in rectangular cell meshes. In Proceedings of the 4th International Conference on Numerical Ship Hydrodynamics (pp. 1–19). [missing publisher/location]

26. ICR. (2010). The World Bank loan: Islamic Republic of Pakistan—Taunsa Barrage Emergency Rehabilitation and Modernization (Economic Internal Rate of Return). [report; missing publisher details]

27. Johnson, M. C., & Savage, B. M. (2006). Physical and numerical comparison of flow over ogee spillway in the presence of tailwater. Journal of Hydraulic Engineering, 132, 1353–1357. https://doi.org/10.1061/(ASCE)0733-9429(2006)132:12(1353)

28. Khan, M. A. (2004). Planning and design of Taunsa Barrage Rehabilitation Project. [missing publisher/institution]

29. Kucukali, S., & Chanson, H. (2008). Turbulence measurements in the bubbly flow region of hydraulic jumps. Experimental Thermal and Fluid Science, 33, 41–53. https://doi.org/10.1016/j.expthermflusci.2008.06.012

30. Longo, S. (2010). Experiments on turbulence beneath a free surface in a stationary field generated by a Crump weir: Free-surface characteristics and the relevant scales. Experiments in Fluids, 49, 1325–1338. https://doi.org/10.1007/s00348-010-0881-5

31. Longo, S. (2011). Experiments on turbulence beneath a free surface in a stationary field generated by a Crump weir: Turbulence structure and correlation with the free surface. Experiments in Fluids, 50, 201–215. https://doi.org/10.1007/s00348-010-0921-1

32. Ma, F., Hou, Y., & Prinos, P. (2001). Numerical calculation of submerged hydraulic jumps. Journal of Hydraulic Research, 39(5), 493–503. https://doi.org/10.1080/00221686.2001.9628274

33. Ma, G., Chen, J., & Yang, W. (2001). Numerical simulation of submerged hydraulic jumps downstream of sluice gates. Journal of Hydraulic Engineering, 127(11), 978–986.

34. Macián-Pérez, J. F., García-Bartual, R., Huber, B., Bayon, A., & Vallés-Morán, F. J. (2020). Analysis of the flow in a typified USBR II stilling basin through a numerical and physical modeling approach. Water, 12. https://doi.org/10.3390/w12010227

35. Mahmoud, N., Abd El-Haleem, A., & El-Saiad, A. (2013). Energy dissipation downstream of the regulators using screens with different hole shapes. Journal of American Science, 9(12), 1–11.

36. Mirzaei, H., & Tootoonchi, H. (2020). Experimental and numerical modeling of the simultaneous effect of sluice gate and bump on hydraulic jump. Modeling Earth Systems and Environment, 6, 1991–2002. https://doi.org/10.1007/s40808-020-00835-5

37. Mukha, T., Almeland, S. K., & Bensow, R. E. (2022). Large-eddy simulation of a classical hydraulic jump: Influence of modelling parameters on the predictive accuracy. Fluids, 7, 1–22. https://doi.org/10.3390/fluids7030101

38. Murzyn, F., & Chanson, H. (2009). Experimental investigation of bubbly flow and turbulence in hydraulic jumps. Environmental Fluid Mechanics, 9, 143–159. https://doi.org/10.1007/s10652-008-9077-4

39. Nikmehr, S., & Aminpour, Y. (2020). Numerical simulation of hydraulic jump over rough beds. Periodica Polytechnica Civil Engineering, 64, 396–407. https://doi.org/10.3311/PPci.15292

40. Ohtsu, I., Yasuda, Y., & Ishikawa, M. (1999). Submerged hydraulic jumps below abrupt expansions. Journal of Hydraulic Engineering, 125(5), 492–499. https://doi.org/10.1061/(ASCE)0733-9429(1999)125:5(492)

41. Rajaratnam, N. (1965). Submerged hydraulic jumps. Journal of the Hydraulics Division, ASCE, 91(HY4), 71–96. https://doi.org/10.1061/JYCEAJ.0001296

42. Rajaratnam, N., & Hurtig, M. (2000). Screen-type energy dissipator for hydraulic structures. Journal of Hydraulic Engineering, 126(4), 310–312. https://doi.org/10.1061/(ASCE)0733-9429(2000)126:4(310)

43. Rajaratnam, N., & Subramanya, K. (1967). Velocity and pressure distribution downstream of a submerged sluice gate. La Houille Blanche, (6), 693–702. [verify pages/year formatting vs your other entry]

44. Sadeghfam, S., Akhtari, A. A., Daneshfaraz, R., & Tayfur, G. (2015). Experimental investigation of screens as energy dissipaters in submerged hydraulic jump. Turkish Journal of Engineering and Environmental Sciences, 38(2), 126–138.

45. Sadeghfam, S., Rajaratnam, N., & Azimi, A. H. (2015). Energy dissipation by submerged permeable screens in stilling basins. Journal of Hydraulic Engineering, 141(5), 04014084.

46. Savage, B. M., & Johnson, M. C. (2001). Flow over ogee spillway: Physical and numerical model case study. Journal of Hydraulic Engineering, 127(8), 640–649. https://doi.org/10.1061/(ASCE)0733-9429(2001)127:8(640)

47. Siuta, T. (2018). The impact of deepening the stilling basin on the characteristics of hydraulic jump. Czasopismo Techniczne, 173–186. https://doi.org/10.4467/2353737XCT.18.046.8341

48. Smith, C. D. (1989). The submerged hydraulic jump in an abrupt lateral expansion. Journal of Hydraulic Research, 27(2), 257–266. https://doi.org/10.1080/00221688909499185

49. Tiwari, A. K., & Seema. (2013). Design of stilling basin models with intermediate sill. Journal of Science, Technology and Management, 2(4), 66–71.

50. Tiwari, A. K., Gahlot, V., & Sharma, A. (2014). Effect of intermediate sill on the performance of stilling basin model. International Journal of Scientific Engineering and Technology, 3(4), 414–417.

51. Tiwari, A. K., & Seema. (2014). Effect of intermediate sill geometry and location on energy dissipation in stilling basins. Journal of Civil Engineering and Construction, 3(1), 1–7.

52. Tiwari, A. K., & Seema. (2014). Performance of stilling basins with end sills of different geometries. International Journal of Civil Engineering Research, 4(2), 167–174.

53. Torkamanzad, N., Hosseinzadeh Dalir, A., Salmasi, F., & Abbaspour, A. (2019). Hydraulic jump below abrupt asymmetric expanding stilling basin on rough bed. Water, 11(9), 1756. https://doi.org/10.3390/w11091756

54. Torkamanzad, S., Kianoush, M. R., & Tajalli, M. (2019). Hydraulic jump in an abruptly expanding asymmetric stilling basin: Experimental assessment of roughness and asymmetry effects. Journal of Hydraulic Engineering, 145(10), 04019045.

55. Wang, H., & Chanson, H. (2015). Experimental study of turbulent fluctuations in hydraulic jumps. Journal of Hydraulic Engineering, 141, 04015010. https://doi.org/10.1061/(ASCE)HY.1943-7900.0001010

56. Wang, Y., Wang, B., Zhang, H., Wang, Z., Zhou, S., & Ye, L. (2016). Three-dimensional numerical simulation on stilling basin of sluice in low head. In [Conference/Proceedings title missing] (pp. 503–509). https://doi.org/10.2991/iccahe-16.2016.84

57. Wu, S., & Rajaratnam, N. (1996). Transition from hydraulic jump to open channel flow. Journal of Hydraulic Engineering, 122, 526–528.

58. Yakhot, V., Thangam, S., Gatski, T. B., Orszag, S. A., & Speziale, C. G. (1991). Development of turbulence models for shear flows by a double expansion technique. Physics of Fluids A: Fluid Dynamics, 4, 1510–1520.